FUNDAMENTALS OF

BioMEMS and Medical Microdevices

Steven S. Saliterman

WILEY-INTERSCIENCE

SPIE PRESS

Bellingham, Washington USA

Chapter 5

Microfluidic Principles

5.1 Introduction

5.1.1 Microfluidic devices

Microfluidics is the study of transport processes in microchannels. Microfluidic devices are the primary component of most LOC devices and μTAS.

Microfluidic devices may consist of channels, valves, mixers, pumps, filters, and heat exchangers. These components allow metering, dilution, flow switching, particle separation, mixing, pumping, incubation of reaction materials and reagents, and sample dispensing or injection. Microfluidic devices may also incorporate various detection schemes. Eventually such devices will improve throughput of samples, increase accuracy, and lower analysis cost. Microfluidic devices offer the possibility of reducing entire laboratory operations onto single chips with the advantage of smaller reagent volumes, shorter reaction times, and parallel operation. An illustration of these components is shown in Fig. 5.1.

Understanding the physics of fluids at the microscale is essential to understanding and designing microfluidic devices. Silicon, glass, and polymers may be used to manufacture devices. Surface characteristics and modifications become important as individual applications are considered.

The purpose of this chapter is to introduce microfluidic device fabrication, microfluidic flow, electrokinetics, and some of the components found in microfluidic devices. These concepts are necessary to understand the LOC devices introduced in Chapter 9, *Micro-Total-Analysis Systems.*

For those interested in designing microfluidic devices the following textbooks should be considered:

Munson, Young, and Okiishi's *Fundamentals of Fluid Mechanics* (2001) or the abridged *A Brief Introduction to Fluid Mechanics* are excellent resources for studying fluid mechanics generally [Young et al., 2001]. Nguyen and Wereley's *Fundamentals and Applications of Microfluidics* (2002) and Francis E.H. Tay's

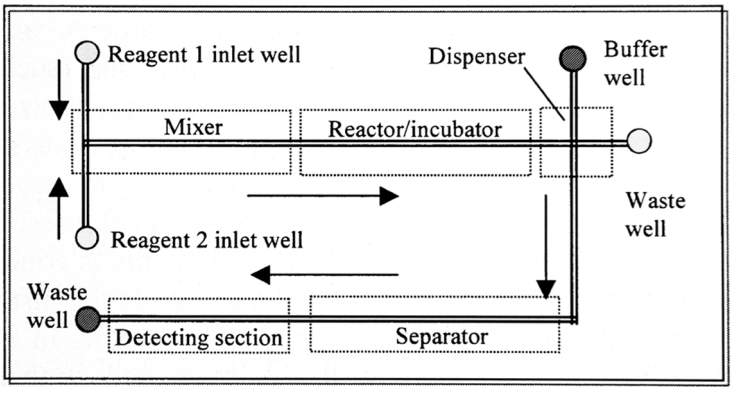

Figure 5.1 Components that may be found in a LOC microfluidic device. [Reprinted with permission from Li (2004), copyright Elsevier.]

Microfluidic and BioMEMS Applications (2002) introduce fabrication techniques for microfluidic devices and fluid mechanics at the microscale.

Dongqing Li's *Electrokinetics in Microfluidics* (2004) covers in-depth the essentials of the electrical double layer, electro-viscous effects, electro-osmosis, electrophoresis, and effects of surface heterogenicity on electrokinetic flow.

5.1.2 History

The expression "miniaturized total chemical analysis systems" was introduced in 1990 by Manz et al. to describe advantages in chromatography and electrophoretic separation by use of "smaller channel inner diameter" devices. Manz later described application of photolithographic techniques for fabrication and the relevance of *electro-osmotic flow* (EOF) to the separation process [Manz et al., 1991; Manz, 1997]. At about the same time Verpoorte reported fabrication of small-volume flow cells for detection purposes, made of microfabricated silicon [Verpoorte et al., 1991 and 1992].

The total-chemical-analysis system (TAS) concept dates back to the 1980s in the quest to simplify the process steps for analytical chemistry. The desire was to have samples *flow* from one step to the next without manipulation by hand [Verpoorte and De Rooij, 2003]. What was once accomplished with multiple lengths of Tygon tubing and plastic connectors is now done within a microfluidic chip.

Chip-based *capillary electrophoresis* (CE) devices were among the earliest microfluidic devices, and brought into focus the need to understand materials and physics of the microenvironment, challenges for manufacturing, and potential for LOC devices. It was recognized that electric fields used for separating species electrophoretically also cause a bulk flow of liquids, or *electro-osmosis.*

Already understood techniques for fabrication of silicon and glass were applied to early microfluidic devices, and invigorated a desire to understand flow, electrokinetics, and surface properties of materials; and how to alter material properties of EOF for analyte separation.

5.1.3 Current scientific interest

Conferences on microfluidics are presently sponsored by a number of professional organizations including the Institute of Electrical and Electronic Engineers (IEEE), American Society of Mechanical Engineers (ASME), International Society for Optical Engineering (SPIE), and the American Institute of Chemical Engineers (AIChe).

The medical market for microfluidic devices dominates all other uses, and includes bioMEMS devices for medical diagnosis, genetic sequencing, chemistry production, drug discovery, and proteomics. Figure 5.2 shows the estimated sales of microfluidic components compared to other MEMS.

Numerous "components" are in the microfluidic designer's toolbox, including microducts, micronozzles, micropumps, microturbines, microvalves,

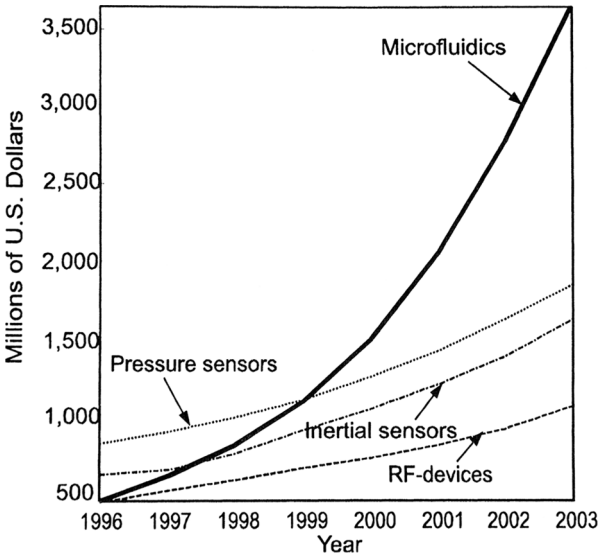

Figure 5.2 Estimated sales of microfluidic components compared to other MEMS devices. [Reprinted with permission from System Planning Corporation (1999), copyright System Planning Corporation.]

microsensors, microfilters, microneedles, micromixers, microreactors, microdispensers, and microseparators.

Glass is an attractive material for microfluidic devices because it is transparent to visible light, it is nonfluorescent, and has EOF properties that can be modified and suppressed. Certain applications, like the *polymerase chain reaction* (PCR), require high-temperature cycling requirements that are not suitable for many acrylic materials. A gradual transition from glass to polymers for some applications has taken place for reasons of lower cost, ease of fabrication, and desired physical properties.

5.1.4 Fabrication

The science of microfluidics includes specialized fabrication techniques, physical properties of fluids and materials at the micro scale, electrokinetic effects, and controlled reaction of reagents and samples.

A number of microfluidic devices are shown in Figs. 5.3 and 5.4. Microfluidic devices are used for LOC devices and μTAS. Microfluidic devices serve to manipulate a fluid and its constituents (sample), and may include biological materials.

The fabrication techniques are largely based on the techniques described in Chapters 2 and 3. A few additional techniques are described below.

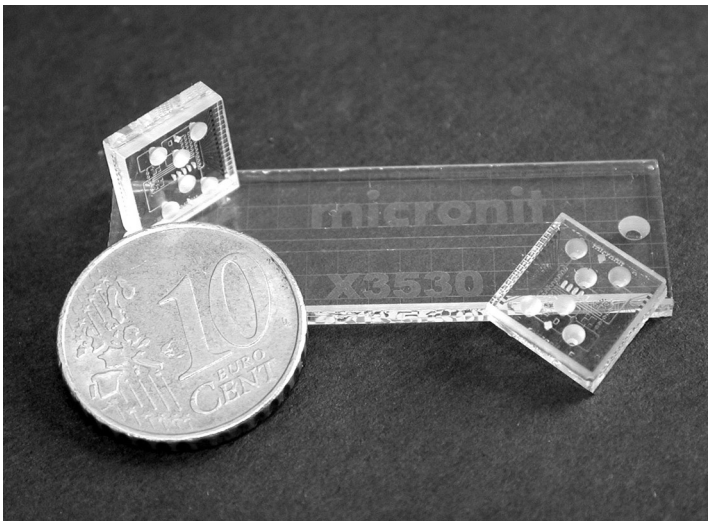

Figure 5.3 Various glass microfluidic chips. (Photo courtesy of Micronit, Inc.)

5.1.4.1 Glass and quartz materials

A number of glass materials have been used for microfluidic devices, including soda-lime glass, borosilicate glass, and quartz. In the simplest of methods, patterning is accomplished with photolithographic techniques to prepare for hydrofluoric acid etching of channels. Holes may be drilled, etched, or powder blasted; and cover plates anodically bonded to convert open channels into closed conduits and chambers. A drawback of quartz is that it requires higher temperatures to bond. More precise channel geometries require surface micromachining techniques as described below.

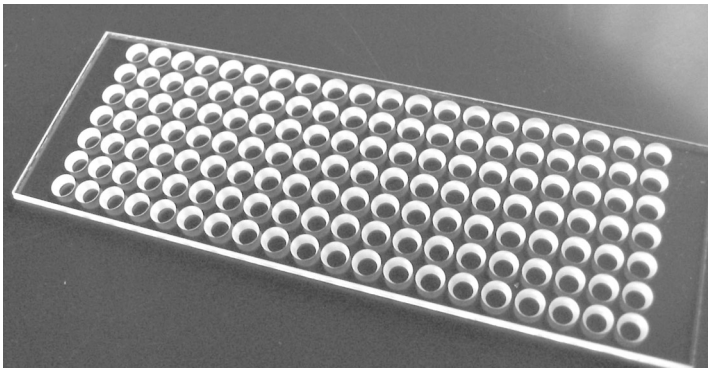

Figure 5.4 Glass microtiter plate. (Photo courtesy of Micronit, Inc.)

5.1.4.2 Silicon techniques

Many techniques may be used to incorporate silicon as substrate or sacrificial material for microchannel fabrication. Among the simplest methods of creating channels is to first etch troughs (isotropically or anisotropically) and vias (holes) in silicon or glass, and then anodically bond a silicon or glass cover. The following examples demonstrate other surface micromachining techniques, most of which overcome the heat, pressure, and electrical requirements of substrate bonding.

Figure 5.5 demonstrates four methods for micromachining channels. The first method involves deposition of a structural material on a sacrificial layer patterned for the desired channel. The sacrificial layer is removed and the open channel sealed by a second deposition of a structural material. The second technique uses the HEXIL process, where a silicon mold is fabricated using bulk micromachining and a sacrificial oxide layer is deposited on the inner wall of the mold wafer. Next, polysilicon is deposited to define the channel wall and the silicon dioxide layer is then etched away releasing the polysilicon channel. The third technique shows the fabrication of a thin nitride/oxide-on-glass channel.

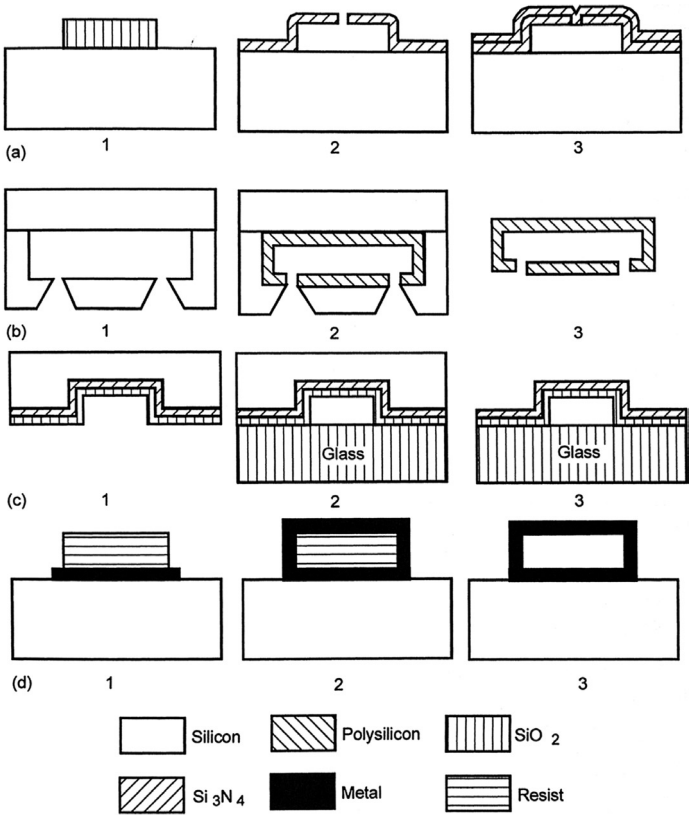

Figure 5.5 Surface-micromachined channels: (a) polysilicon; (b) molded silicon channel; (c) oxide/nitride channel; and (d) metal channel. [Reprinted with permission from Nguyen and Wereley (2002), copyright Artech House.]

A nitride/oxide double layer is deposited on the channel walls of a bulk micromachined silicon substrate. The structure is then anodically bonded to a glass wafer. By etching away the silicon, a thin nitride/oxide-on-glass channel remains. In the last technique, a metal channel is created by depositing a metal "seed" layer on the silicon substrate and electroplating it to define the channel bottom thickness. A photoresist such as AZ4620 is deposited to form a thick-film sacrificial layer. Gold is then sputtered on the resist structure as the second seed layer, and further electroplating defines the side walls and top of the channel. Acetone may be used to remove the sacrificial resist layer.

Silicon material is generally advantageous for applications with strong solvents, high temperatures, and chemically stable surfaces. Because silicon is conductive it is less advantageous for microfluidic devices because of interference with high electric fields used in electrophoretic separation (fields are limited to $\sim$10 V/cm, which results in slow separation). This problem may be reduced by insulator improvements and the use of different dimensions [Bousse et al., 2000].

Other drawbacks of silicon for microfluidics include costly manufacturing equipment, labor intensity that requires specialized skills, optical opacity of silicon, difficulty of component integration, and surface characteristics are not well suited to biological problems.

5.1.4.3 Polymeric surface micromachining

Polymer devices offer the advantage of lower cost per unit produced, and are suitable for mass production and disposable devices. Microfluidic devices may be fabricated by techniques described previously, including LIGA, thick resist lithography, soft lithography, microstereolithography (MSL), and micromolding. *Laser ablation* has also been used to create very precise, well-defined channels, and may be useful for multilayer channel networks. Channels may be sealed by laminating with thin films of poly(ethylene terephthalate) and polyethylene adhesive.

Polymeric surface micromachining is another way to fabricate with polymers. Polymers may be used as structural or sacrificial material. Polyimide (PI) photoresist is commercially available as Proimide 348 or 349 (Ciba Geigy) or PI-2732 (DuPont). Thicknesses to 40 μm may be obtained by spinning, and may be used for thick-resist patterning. It can be etched with RIE in oxygen plasma.

PI is also a good substrate material. Aluminum, titanium, and platinum can be sputtered onto it. Using photolithography, RIE, and thin-film lamination, it is possible to form complex channel structures with metal electrodes.

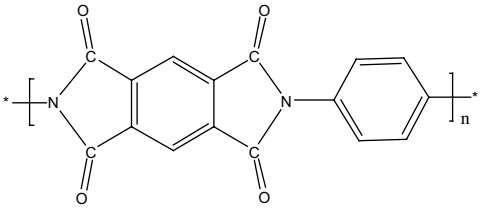

Polyimide (PI)

Parylene is a polymer that can be deposited with CVD at room temperature. Conformal coatings of several micrometers to several millimeters may be deposited. Parylene N is a good dielectric, exhibiting very low dissipation factor, high dielectric strength, and a frequency independent dielectric constant. Parylene C has very low permeability to moisture and corrosive gases, and is used for conformal insulation. Parylene D has the added ability of withstanding high temperatures.

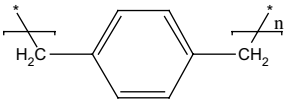

Parylene N

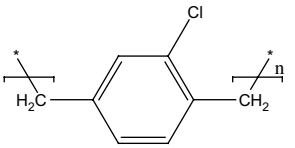

Parylene C

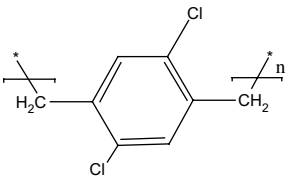

Parylene D

Parylenes may be deposited as fast as 10 μ/min (parylene C), and may be used as structural material. It is a soft material with a low Young's modulus and is useful for microvalves and micropumps. Parylene coatings also improve biocompatibility [Nguyen and Wereley, 2002].

5.2 Transport Processes

5.2.1 Introduction

The small scale of microfluidics results in changes in fluid behavior. Since typically only the area where fluid is processed (the *flow stream* for analysis) needs to be miniaturized, emphasis can be given to these components.

Some bioMEMS devices of the future may be more like the *Mars Exploration Rover*. Rather than being launched to a distant planet, they may be attached to the skin, implanted, or move about inside the body; passively or actively obtaining samples with microneedles, diffusive surfaces or flow-through ports. They may be self-powered for extended periods, operate in a harsh environment, and perform their function by remote control. In such instances the entire system may be miniaturized. The size of microfluidic devices is shown comparatively in Fig. 5.6.

Lab-on-a-chip devices primarily transport liquids, including whole blood, serum (containing proteins and other chemistries), bacterial suspensions, and various reagents and buffers. These devices mostly control flow, mass transport, and heat transfers in microchannels.

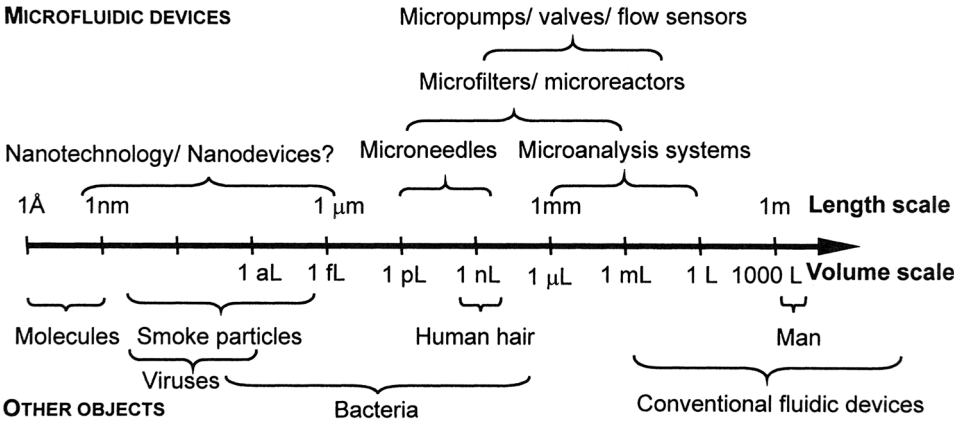

Figure 5.6 Dimensional comparison of bioMEMS components with more familiar objects. [Reprinted with permission from Nguyen and Wereley (2002), copyright Artech House.]

Transport processes may be generally classified into three categories according to the characteristic dimension, L_C of the system: (1) macroscale systems: $L_C > 200$ μm. (2) microscale systems: 100 nm $< L_C <$ 200 μm. (3) nanoscale systems: $L_C < 100$ nm. Characteristics of the transport processes change significantly as the characteristic dimension of the system changes from one category to the next [Li, 2004].

In LOC devices, where fluids with significantly different molecular content may interact, significant gradients of molecular and cellular content within the fluid may occur. Moreover, certain bioMEMS devices such as tissue scaffolding systems may intentionally create gradients for cell growth, including nutritional supply, drugs, and oxygenation. *Classical fluid dynamics* considers the macroscopic properties of a fluid and considers the fluid characteristics to vary continuously throughout the fluid, or *continuum.* Alternatively, a more complicated molecular approach to fluid mechanics may be required, in which the state (i.e., position and velocity) of each molecule is followed over time.

There are two general approaches in analyzing fluid-mechanics problems. The first is the *Eulerian method*, which uses *field concepts* and considers properties of pressure, density, velocity, etc., as functions of space and time. It is possible to understand *flow* in terms of what happens at fixed points in space as fluid passes those points. The second is the *Lagrangian method* in which individual particles are followed as they move about over time [Young et al., 1997].

Flow maybe influenced by kinematic properties (velocity, viscosity, acceleration, vorticity), transport properties (viscosity, thermal conductivity, diffusivity), thermodynamic properties (pressure, thermal conductivity, density), and other properties (surface tension, vapor pressure, surface accommodation coefficients) [Nguyen and Wereley, 2002].

5.2.2 Sample size

Sample size plays a role in designing LOC devices, and it is worth spending a moment to consider what effect reduced volumes has on the number of analyte targets available for study. Concentration of a sample determines how many target molecules are present. Since smaller volume means less analyte is present, it is necessary to think about how much sample is necessary to adequately perform an analysis given the level of detector ability. The relationship between sample volume (V) and analyte concentration is

$$V = \frac{1}{\eta_s N_A A_i}, \tag{5.1}$$

where

η_s is the sensor efficiency $0 \leq \eta_s \leq 1$,
N_A is 6.02×10^{23}, or Avogadro's number, and
A_i is the concentration of analyte, i.

The concentration of typical analytes in blood is shown in Fig. 5.7. If a sample size is too small it may not contain the analyte of interest. The required analyte concentration/sample volume ratio for clinical chemistry assays, immunoassays, and DNA probe assays is shown in Fig. 5.8.

Immunoassays with lower analyte concentrations require sample volumes on the order of *nanoliters*, while preconcentrated analysis of DNA present in blood requires sample volumes of the order of a *milliliter*. This is why amplification techniques such as the PCR for DNA are necessary to detect minute amounts of DNA material related to disease conditions.

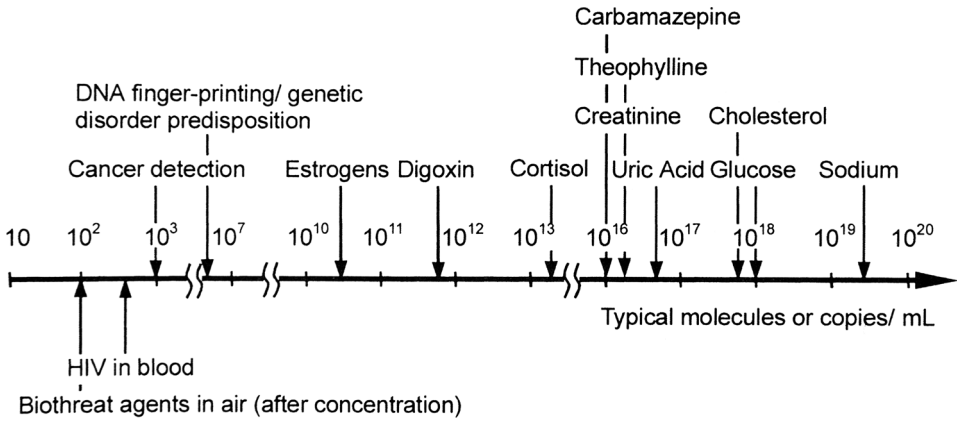

Figure 5.7 Concentrations of typical diagnostic analytes in human blood or other samples. [Reprinted with permission from Peterson et al. (1999), copyright Springer.]

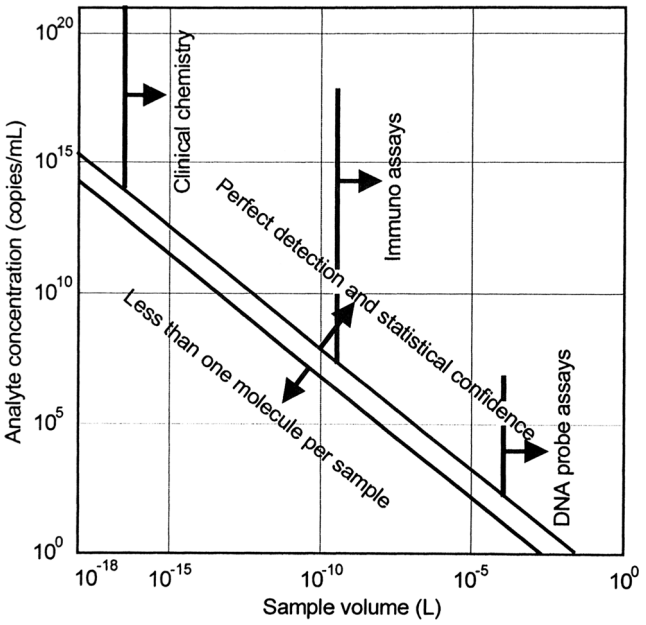

Figure 5.8 Required analyte concentration/sample volume ratio for clinical chemistry assays, immunoassays, and DNA probe assays. [Reprinted with permission from Peterson et al. (1999), copyright Springer.]

5.2.3 What is a fluid?

A fluid is a substance that deforms continuously under the application of shear (tangential) stress of any magnitude. This includes gases and liquids. Consider a solid block of material as illustrated in Fig. 5.9. A shearing force deforms the object, but it returns to its original shape so long as the elastic limit is not exceeded. In contrast, a fluid between two plates deforms and stays deformed once the shearing force is removed.

A fluid is said to be *Newtonian* if the shear stress (shear force/area fluid contact) is directly proportional to the rate of strain (du/dy) within the fluid.

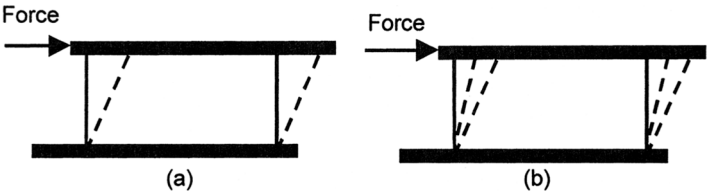

Figure 5.9 When both a solid (a) and liquid (b) are subjected to a shearing force, the solid returns to its original or equilibrium position, while the liquid remains deformed. [Reprinted with permission from Nguyen and Wereley (2002), copyright Artech House.]

Most fluids and gases are Newtonian, and this is assumed in the discussion that follows.

The *viscosity* of a fluid is an additional property that must be considered. For example, if a fluid is placed between two parallel plates, and a shearing stress is applied to the upper plate, the fluid deforms continuously. However, fluid in contact with the upper plate moves with the plate velocity, while the fluid in contact with the lower plate has zero velocity (a *no-slip condition*). The linear variation of shearing stress with rate of shearing strain may be plotted for different fluids encountered in microfluidic applications and referenced from published tables.

For common fluids (e.g., water, oil, and air) the relationship takes the following form:

$$\tau = \mu \frac{du}{dy}, \tag{5.2}$$

where

τ is the shearing stress,
μ is the absolute or dynamic viscosity, and
du/dy is the velocity gradient.

Flow fields in which the shearing stresses are assumed to be negligible are said to be *inviscid* or frictionless.

Other definitions of importance include the *kinematic viscosity* of a fluid, which relates the absolute viscosity to density:

$$\nu = \frac{\mu}{\rho}, \tag{5.3}$$

where

ν (the Greek symbol *nu*) is the kinematic velocity (m^2/s), and
ρ is the density or mass per unit volume;

the *specific weight* of a fluid, which is defined as the weight per unit volume:

$$\gamma = \rho g, \tag{5.4}$$

where

g is the local acceleration due to gravity;

and the *specific gravity* (SG) of a fluid, which is the ratio of the density of the fluid to the density of water at some specified temperature [Young et al., 2001]:

$$\mathrm{SG} = \frac{\rho}{\rho_{H_2O@4^\circ C}}. \tag{5.5}$$

5.2.4 Laminar flow

Flow can be considered as being laminar, transitional, or turbulent, and is dependent on the fluid density and viscosity, characteristic velocity, geometry of

the channel, and whether or not the flow is past an object. For most simple microfluidic channels in which the width and height are less than 1 mm and velocities less than a centimeter per second, the flow will be laminar [Bousse et al., 2000].

Modeling flow in microfluidic channels is by no means simple, and computational methods should be gleaned from the literature based on the specific application. The presentation here of *Poiseuille flow* in a tube does, however, serve to introduce the basic concepts of laminar flow and viscosity.

5.2.4.2 Reynolds number

Flow patterns will typically be functions of *Reynolds number*, a measure of the ratio between inertial forces and viscous forces in a particular flow. This dimensionless value is defined as

$$\mathrm{Re} = \frac{\rho V D}{\mu}, \tag{5.6}$$

where

ρ is the fluid density,
V is the mean fluid velocity,
D is the pipe diameter, and
μ is the fluid viscosity.

In circular tube flows without obstruction, conventional fluid mechanics would dictate that Reynolds numbers smaller than about 2,100 typically indicate laminar flow, while values greater than 4,000 are turbulent. Between these numbers the flow may switch between laminar and turbulent conditions, and is considered *transitional.*

In microfluidic systems flow, transition in rectangular channels may occur with Reynolds number between 200–700, possibly as a consequence of hydraulic diameter or aspect ratio [Peng et al., 1994].

Very low Reynolds numbers $\ll 1$ may be encountered in microfluidic systems. For example, for water (viscosity of 10^{-3} kg/(s m), density of 10^{3} kg/m^{3}), moving through a channel with diameter of 10 μm, at a velocity of 1 mm/s, the Reynolds number is 10^{-2}. Contrast this to a channel with diameter of 100 μm and fluid velocity of 10 m/s, where the Reynolds number is 1,000 [Nguyen and Wereley, 2002].

5.2.4.3 Fluid kinematics

Fluid kinematics allows for discussion of various aspects of fluid motion without being concerned about the forces that induce the motion. A *field representation* of flow is the representation of fluid parameters as functions of *spacial coordinates* and *time.* Considerable information about flow can be obtained from the *velocity*

and acceleration fields; the former are considered here. The velocity field in steady state is defined as

$$\mathbf{V} = u(x, y, z, t)\hat{\mathbf{i}} + v(x, y, z, t)\hat{\mathbf{j}} + w(x, y, z, t)\hat{\mathbf{k}}, \tag{5.7}$$

where

u, v, w are the x, y, and z components of the velocity vector, and
t is time.

For problems related to flow in most microchannels, we can consider that one or two of the velocity components will be small relative to the others, and reduce the problem to 1D or 2D flow.

The velocity of a particle is the *time rate of change* of the position vector for that particle. The *position vector* $\mathbf{r}_A$ is the position of a particle relative to a coordinate system (Fig. 5.10). The time derivative of this position gives the velocity of the particle:

$$d\mathbf{r}_A/dt = \mathbf{V}_A. \tag{5.8}$$

The *direction* of the fluid velocity relative to the x axis is given by

$$\tan\theta = \frac{v}{u}. \tag{5.9}$$

By determining $\mathbf{V}$ and θ for several locations in the x-y plane, it is possible sketch the *velocity field.*

In *steady flow* the velocity at a given point in space does not vary with time, unlike in turbulent flow. *Streamlines* are the lines that are tangental to the velocity vectors throughout the flow field. In a steady flow these lines are fixed in space. For a 2D flow the slope of the streamline must be equal to the tangent of the angle that the velocity vector makes with the x axis:

$$\frac{dy}{dx} = \frac{v}{u}. \tag{5.10}$$

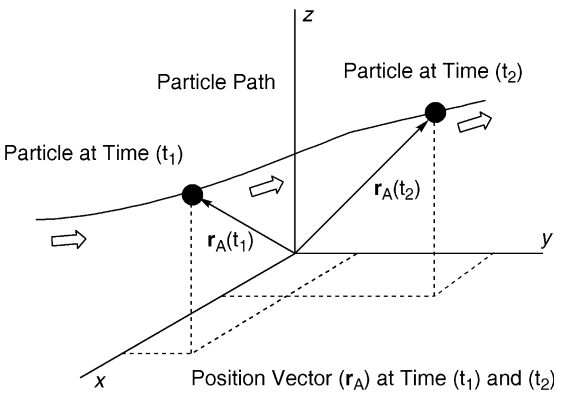

Figure 5.10 Particle location in terms of position vector.

If the velocity field is known as a function of x and y, integration of this equation yields the *equation of streamlines* inclusive of some constant. Various lines can be plotted in the x-y plane for different values of the constant. The *stream function* then is defined as

$$\psi = \psi\,(x, y). \tag{5.11}$$

Streamlines are parallel to the velocity field.

5.2.4.4 Poiseuille flow

We can now consider steady, laminar flow in circular tubes (ignoring entrance effects). This is commonly known as *Hagen-Poiseuille flow* or simply *Poiseuille flow*. The *Navier-Stokes equations* (nonlinear, second order, partial differential equations) are the governing differential equations of motion for incompressible Newtonian fluids, and derive from *three equations of motion* and *conservation of mass equation*. Poiseuille flow is an example of an exact solution to the Navier-Stokes equations, which reveals that at any cross section the velocity distribution of the fluid is *parabolic*.

This velocity distribution is expressed as

$$v_z = \frac{1}{4\mu}\left(\frac{\partial p}{\partial z}\right)(r^2 - R^2), \tag{5.12}$$

where

μ is the fluid viscosity,
$\partial p/\partial z$ is the z component of the pressure gradient,
r is the distance from the center of the tube, and
R is the radius of the tube.

The *maximum velocity* is at the pipe center, and the *minimum velocity* (zero) is at the pipe wall. Every part of the fluid at a given r can be visualized as moving along its own path line parallel to the tube wall, but at a slightly different velocity than the neighboring path line (Fig. 5.11). Shear stress is the consequence of the velocity variation and fluid viscosity.

Fully developed horizontal tube flow is a balance between pressure and viscous forces, or

$$\frac{\Delta p}{\ell} = \frac{2\tau}{r} \quad \text{or} \quad \tau = \frac{\Delta p r}{2\ell}. \tag{5.13}$$

The shear stress is maximum at the wall (*wall shear stress*), and zero at the centerline. The shear stress distribution through the tube is a linear function of the radial coordinate

$$\tau = \frac{2\tau_w r}{D}, \tag{5.14}$$

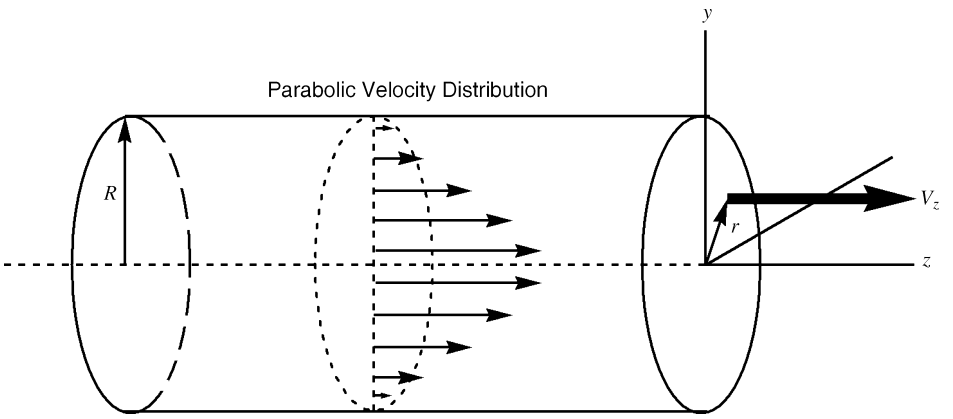

Figure 5.11 Velocity distribution in steady laminar flow in a circular tube.

where

τ_w is the wall shear stress, and
D is the diameter.

Combining the previous two equations, the pressure drop and wall shear stress are then seen to be related as follows:

$$\Delta p = \frac{4\ell\tau_w}{D}. \tag{5.15}$$

For laminar flow of a Newtonian fluid the shear stress is proportional to the velocity gradient:

$$\tau = -\mu\frac{du}{dr}. \tag{5.16}$$

It then follows that

$$\frac{du}{dr} = -\left(\frac{\Delta p}{2\mu\ell}\right)r, \tag{5.17}$$

and integration yields the velocity profile:

$$\begin{aligned} \int du &= -\frac{\Delta p}{2\mu\ell}\int r\, dr, \\ u &= -\left(\frac{\Delta p}{4\mu\ell}\right)r^2 + C_1, \end{aligned} \tag{5.18}$$

where

C_1 is a constant.

Recall that velocity equals zero at the wall and $r = D/2$, allowing calculation of the constant:

$$C_1 = \frac{\Delta p D^2}{16\mu\ell}. \tag{5.19}$$

The *velocity profile* can now be written as

$$u(r) = \left(\frac{\Delta p D^2}{16\mu\ell}\right)\left[1 - \left(\frac{2r}{D}\right)^2\right] = V_c\left[1 - \left(\frac{2r}{D}\right)^2\right], \tag{5.20}$$

where

V_c is the maximum or centerline velocity.

The *volume flowrate* through the pipe can be obtained by integrating the velocity profile across the pipe, and results in

$$Q = \frac{\pi R^2 V_c}{2}, \tag{5.21}$$

and the *average velocity* is the flowrate divided by the cross sectional area:

$$V = \frac{Q}{A} = \frac{Q}{\pi R^2} = \frac{\pi R^2 V_c}{2\pi R^2} = \frac{V_c}{2} = \frac{\Delta p D^2}{32\mu\ell}, \tag{5.22}$$

where

Δp is the pressure drop over length, ℓ along the tube, and
D is the diameter.

The relationship between the volume rate of flow, Q, passing through the tube and the pressure gradient is known as *Poiseuille's law*, and is determined as follows:

$$Q = \frac{\pi D^4 \Delta p}{128\mu\ell} = \frac{\pi R^4 \Delta p}{8\mu\ell}. \tag{5.23}$$

For a given pressure drop per unit length, the volume flow rate is inversely proportional to the viscosity and proportional to the tube radius to the fourth power. Doubling of the tube radius produces a sixteen-fold increase in flow [Young et al., 2001].

5.2.5 Surface area to volume

Surface area to volume (SAV) increases significantly as dimensions are reduced for microfluidic channels. For example, for a circular microchannel 100 μm in diameter, the SAV ratio is:

$$\text{SAV} = \frac{2\pi rL}{\pi r^2 L} = \frac{2}{r} = 4 \times 10^4 \text{ m}^{-1}, \tag{5.24}$$

where

r is the radius, and
L is the length.

As the SAV increases, processes such as capillary electrophoresis becomes more efficient due to easier removal of heat, and transport due to electrokinetic flow decreases because of rapid diffusion of macromolecules and adsorption to channel surfaces.

5.2.6 Diffusion

In laminar flow, two or more streams flowing in contact with each other mix only by diffusion. This is not advantageous when mixing is desirable, in which case some form of passive or active mixing is required.

Particle movement by *Brownian motion* causes particles to spread out over time so that the average concentration of particles throughout the volume is constant. The mean square displacement of a particle from its origin is proportional to time:

$$\bar{x}^2 = 2Dt, \tag{5.25}$$

where

x is the distance a particle moves,
t is the amount of time, and
D is the diffusion coefficient.

The diffusion coefficient (D) is defined as

$$D = \frac{RT}{6\pi r\eta N_{\mathrm{A}}}\left[1 + C\left(\frac{\partial \ln y}{\partial C}\right)_{T,P}\right], \tag{5.26}$$

where

R is the gas constant,
T is temperature,
r is particle radius,
N_{A} is Avogadro's number,
C is concentration in moles/liter,
η is the solution viscosity, and
y is the activity coefficient in moles/liter.

Since distance varies to the square power, diffusion becomes very important on the microscale. For example, Hgb ($D = 10^{-7}\mathrm{cm}^2\ \mathrm{s}^{-1}$) takes 10^6 seconds to diffuse 1 cm, but only 1 second to diffuse 10 μm. Therefore, in a 1-cm wide tube, diffusion of hemoglobin is not usually an important consideration, but in a microchannel 10-μm wide, the distance traveled due to diffusion becomes important [Beebe et al., 2002].

The optimal size domain for microfluidic channel cross sections is somewhere between 10 μm and 100 μm. At smaller dimensions detection is too difficult and at greater dimensions unaided mixing is too slow. Therefore, the typical cross section diameter is $\sim 2 \times 10^{-3}$ mm^2, and the flow range is 1–20 nL/s. When diluting an assay component, the two flows must be controlled within $\sim 1\%$, or pL/sec range [Bousse et al., 2000].

The present simulation tools for studying diffusion-based mixers are often slow and poorly suited to the special geometry of micro-channels. Stay and Barocas (2004) derive the necessary conditions for a reduced-dimensional model of flow and diffusion in a thin channel (i.e., the height is much less than the width).

5.3 Electrokinetic Phenomena

5.3.1 Introduction

Electrokinetic phenomena in microfluidics include electro-osmosis, electrophoresis, streaming potential, and dielectrophoresis. Harnessing electrokinetic phenomena in microfluidic devices for moving fluid and particles (including proteins, cells, bacteria and viruses) is essential for μTAS and other LOC applications.

In *electro-osmosis*, fluid can be made to move relative to a stationary charged or conducting surface through application of an electric field. Application of the electric field induces formation of the *electric double layer* (EDL). The EDL consists of the *charged surface* and the *compact* liquid layer containing the *immobile balancing charges*, and a *diffuse* liquid layer of *mobile ions.* From the compact layer to the electrically neutral bulk liquid, the net charge density gradually reduces to zero (Fig. 5.12). The compact layer is several angstroms thick (one angstrom is equal to 10^{-10} m). The *shear plane* is the boundary between the compact layer and the diffuse layer (where the liquid velocity is zero). When an electric

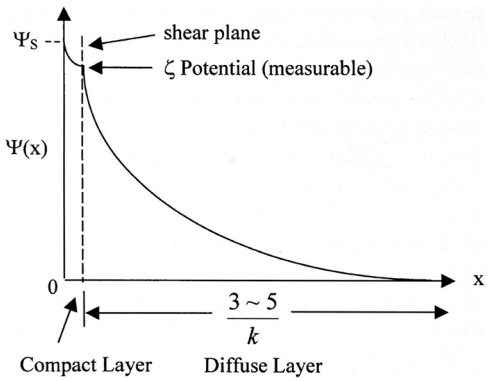

Figure 5.12 The electric double layer (EDL) potential field for a flat surface in contact with an aqueous solution. [Reprinted with permission from Li (2004), copyright Elsevier.]

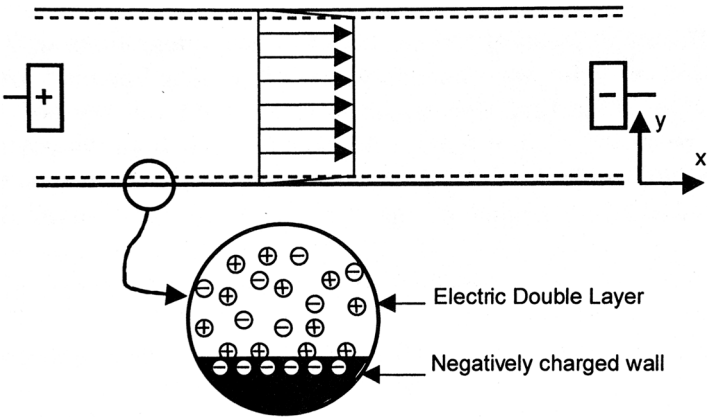

Figure 5.13 Representation of the flow in a constant cross-section channel during electro-osmotic flow. [Reprinted with permission from Nguyen and Wereley (2002), copyright Artech House, 2002.]

field is applied, the excess counterions in the diffuse layer move under the applied electric force; this is called *electro-osmosis. Electro-osmotic flow* (EOF) occurs when the moving ions drag the surrounding fluid with them due to the viscous effect, creating "bulk flow." Figure 5.13 shows the flow in a constant cross section channel undergoing EOF.

Electrophoresis is the motion of an electrostatically charged particle (solid, liquid, or gas) in a bulk liquid phase. In the presence of an electric field the particle can be induced to move relative to the stationary or moving liquid. Electrophoresis is a widely used separation technique.

The *streaming potential* occurs when an aqueous ion containing solution is forced to flow through a capillary or microchannel under an applied hydrostatic pressure in the absence of an applied electric field. An *electroviscous effect* occurs, or resistant to flow.

Next we will consider the mechanisms of each these phenomena, as well as *dielectrophoresis*, the movement of dielectric particles in a spatially nonuniform electric field.

5.3.2 Electro-osmosis

5.3.2.1 Introduction

Most solid–liquid and many liquid–liquid interfaces have an electrostatic charge and consequently an electric field near the interface. These interfacial electrokinetic phenomena are important to microfluidic processes. Most applications use dielectric materials, including plastics, organic liquids, aqueous electrolyte solutions, and gases. Molecules of many dielectric materials are permanently polarized due to their asymmetrical molecular structure. In the presence of an

electric field, molecules of all dielectric materials have a dipole that comprises two equal and opposite charges separated by a distance.

The *Poisson equation* describes the electrical field potential in a dielectric medium [Li, 2004]:

$$\nabla^2\psi = -\frac{\rho}{\varepsilon_r\varepsilon_o}, \tag{5.27}$$

where

ψ is the electrical field potential,
ρ is the free charge density,
ε_r is the dielectric constant of the medium, and
ε_o is the permittivity of a vacuum (8.85×10^{-12} F/m).

When there is no free-charge density, such as in pure organic liquids and neutral aqueous solution, this quantity becomes zero (the *Laplace equation*).

Most materials obtain a surface electric charge when they are brought into contact with an aqueous solution. The origin of the surface charge includes the following:

(1) *Different affinities for ions of different signs to two phases.* This includes for example, (a) the distribution of anions and cations between two immiscible phases such as oil and water, (b) preferential adsorption of certain ions from an electrolyte solution onto a solid surface, and (c) preferential dissolution of ions from a crystal lattice.
(2) *Ionization of surface groups.* For example, materials with acidic groups such as COOH on the surface dissociates in solution leaving COO^- on the surface and H^+ in the aqueous solution. This creates a negatively charged surface. In contrast, materials containing basic groups dissociates leaving positive charges on the surface and OH^- groups in the aqueous solution. Changes in the solution pH changes the surface charge. Most metal oxides have either positive or negative surface charge depending on the bulk pH.
(3) *Charged crystal surfaces.*

Both glass and polymer microfluidic devices tend to have *negatively charged* surfaces (in later chapters we discuss *modification* of these surfaces for improved functionality).

The electrostatic charges on the solid surface attract *counterions* in the liquid. The concentration of these counterions is higher near the surface than in the bulk fluid further away from the surface (Fig. 5.14).

The *Poisson-Boltzmann equation* is used to describe the ion and potential distributions in the diffuse layer. The diffuse layer thickness is dependent on the bulk ionic concentration and electrical properties of the liquid, ranging from several nanometers for high ionic strength solutions, to 1–2 μm for extremely low ionic solutions such as deionized water and pure organic liquids.

The potential at the shear plane is called the *zeta potential* (ζ), and can be measured experimentally. It may be used as an approximation of the surface potential, which is difficult to measure.

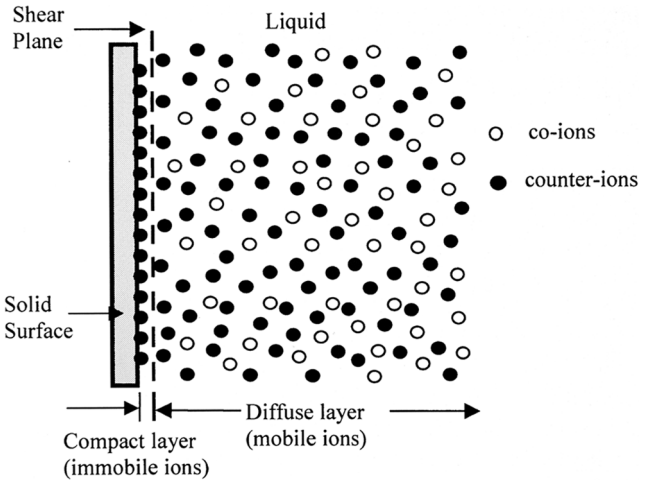

Figure 5.14 The electric double layer (EDL) for a flat surface in contact with an aqueous solution. [Reprinted with permission from Li (2004), copyright Elsevier.]

The distribution of ions near a charged surface can be expressed by the *Boltzmann equation* as follows [Li, 2004]:

$$n_i = n_i^{\infty} \exp\left(-\frac{z_i e\psi}{k_b T}\right), \tag{5.28}$$

where

n_i is the ionic number concentration of type i ion at a given position,
n_i^{∞} is the ionic number concentration of type i ion, infinitely away from the charged surface,
z_i is the value of the ionic valence,
e is the fundamental charge of an electron,
ψ is the electrical field potential (V) at a given position,
k_b is the Boltzmann constant, and
T is the absolute temperature in Kelvin.

Assumptions include that the system is in equilibrium, ions have no macroscopic motion, the system is subjected only to a homogenous surface EDL field, and the charged surface is in contact with an infinitely large liquid medium. At higher fluid flows ($\mathrm{Re} > 10$) the above Boltzmann distribution does not hold.

We will now consider the electric double layer field in terms of the *Poisson-Boltzmann equation* [Li, 2004]:

$$\nabla^2\psi = \frac{2zen_o}{\varepsilon_r\varepsilon_o}\sinh\left(\frac{ze\psi}{k_b T}\right). \tag{5.29}$$

A more general form of the equation considering charge density and inclusive of the bulk ionic concentration and valence of type i ions is as

$$\nabla^2\psi = \frac{e}{\varepsilon_r\varepsilon_o}\sum z_i n_{i\infty}\exp\left(-\frac{z_i e\psi}{k_b T}\right). \tag{5.30}$$

By defining the *Debye-Huckel parameter*:

$$\kappa^2 = \frac{2z^2e^2n_\infty}{\varepsilon_r\varepsilon_o k_b T}, \tag{5.31}$$

and the nondimensional electric potential:

$$\Psi = \frac{ze\psi}{k_b T}, \tag{5.32}$$

we may rewrite the Poisson-Boltzmann equation as

$$\nabla^2\Psi = \kappa^2\sinh\Psi.$$

The Debye-Huckel parameter is independent of the solid surface properties and is determined by the liquid properties of the ionic valence and bulk ionic concentration. The *characteristic thickness* of the EDL is defined as

$$\frac{1}{\kappa}. \tag{5.33}$$

This is shown in Fig. 5.12. The bulk ionic concentration may be expressed in terms of molarity:

$$n_\infty = \left(M\frac{\text{mol}}{\text{L}}\right)\left(1000\frac{\text{L}}{\text{m}^3}\right)\left(N_\text{A}\frac{1}{\text{mol}}\right) = 1000N_\text{A}M, \tag{5.34}$$

and the characteristic thickness of the EDL becomes [Li, 2004]

$$\frac{1}{\kappa} = \left[\frac{\varepsilon_r\varepsilon_o k_b T}{2z^2e^2n_\infty}\right]^{1/2} = \left(\frac{3.04}{z\sqrt{M}}\right)\times 10^{-10}\text{m}, \tag{5.35}$$

where (for pure water at 298°K)

$\varepsilon_r = 78.5$
$\varepsilon_o = 8.85\times 10^{-12}$F/m,
$e = 1.602\times 10^{-19}$C,
$k_b = 1.381\times 10^{-23}$J/K, and
$N_\text{A} = 6.022\times 10^{23}$/mol.

The Debye length varies inversely with the square root of the ion molar concentration.

In *electro-osmosis*, when an electric field is applied, the excess counterions in the diffuse layer of the EDL will move under the applied electrical force. Surrounding liquid molecules are pulled along by a *viscous effect*, resulting in bulk fluid motion, or EOF. Electro-osmotic flow may for example, be calculated for

slit, cylindrical and rectangular microchannels. Calculation of the EDL near flat, spherical and cylindrical surfaces and calculation of the EOF for these various geometries is provided in Li's book. We will consider here for illustration the electro-osmotic flow in a slit microchannel.

In a *slit microchannel* (formed between two parallel plates), where the width is much larger than the height of the channel, the electro-osmotic flow velocity may be determined as follows [Li, 2004]:

$$v_{av} = -\frac{E_z \varepsilon_r \varepsilon_o \zeta}{\mu}, \tag{5.36}$$

where

v_{av} is the average electro-osmotic flow velocity,
E_z is the applied electrical field (V/m),
ε_r is the dielectric constant of the medium,
ε_o is the permittivity of a vacuum,
ζ is the zeta potential at the shear plane, and
μ is the viscosity.

Assumptions in this calculation are that the EDL thickness is small and the electrical field is one-dimensional. Note that electro-osmotic flow velocity is linearly proportional to the applied electrical field strength and zeta potential. In the case of a very thin EDL, zeta is the zeta potential of the channel wall.

5.3.2.2 Advanced modeling

Advanced modeling of electro-osmotic flow includes use of the *modified Navier-Stokes equation* describing the motion of a liquid driven by electrokinetic body forces, the energy equation governing the temperature field due to Joule heating; and ionic concentration distributions that are governed by either the *Nernst-Planck* equation or described by the Boltzmann distribution [Tang et al., 2003]. Additional factors that need to be considered include electro-viscous effects on pressure-driven flow, and surface heterogenicity and roughness [Li, 2004].

Molecular dynamics (MD) simulation may be more useful for studying fluid flow in nanoscale channels. In MD simulation, the ion-ion, ion-wall, and ion-water interactions are calculated explicitly, the trajectory of the system is integrated by using classical mechanics, and ion concentration and bulk velocity are obtained by statistical averaging [Qiao and Aluru, 2003].

A technique for actually mapping fluid flow rates in microfluidic channels with submicron resolution has been reported [Kuricheti et al., 2004]. The technique employs confocal microscopy in conjunction with fluorescence correlation spectroscopy to determine velocity profiles and velocity images in PDMS. Nanometer-scale fluorescent polymer spheres are used as fluid tracers.

5.3.2.3 Implementation

Various electrokinetic techniques for separation chromatography were reviewed by Szumski and Buszewski (2002). An interesting model for displacing one electrolyte with another solution in a microchannel using electro-osmosis was described by Ren et al. (2001).

An ac electro-osmotic pump has been fabricated with flow rates as high as 50 μm/sec in a closed-loop channel. An ac electro-osmotic device is made up of an interdigitated array of unequal-width electrodes located at the bottom of a channel, with an ac voltage applied between the small and large electrodes. The driving forces of ACEOF are the coulombic forces exerted on the double layer above the electrodes due to the tangental component of the electric field (Fig. 5.15).

Liu et al. (2004) discuss the phenomenon that in an electrokinetically operated DNA hybridization chip, oligonucleotides have an electro-osmotic flow that is opposite their electrophoretic motility. By coating the inner walls of a microfluidic system with hexadimentrine bromide (polybrene PB), and other cationic polymers, it is possible to reverse the direction of electro-osmotic flow such that it acts in the same direction as the electrophoretic transport of oligonucleotides.

5.3.3 Electrophoresis

5.3.3.1 Introduction

Electrophoresis is the effect by which charged species in a fluid are moved by an electric field relative to the fluid molecules. The charged species accelerates until the electric force is equal to the frictional force. Recall in electro-osmosis the charged wall is stationary and fluid moves under an applied electric field. In electrophoresis the liquid is stationary, while the particles move under the influence of the electrical charge. Figure 5.16 shows the charge distribution around an electrophoretic particle.

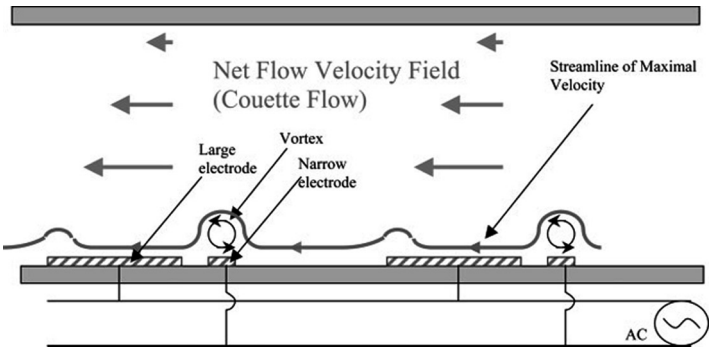

Figure 5.15 Schematic representation of an ACEOF profile. [Reprinted with permission from Debesset et al. (2004), copyright The Royal Society of Chemistry.]

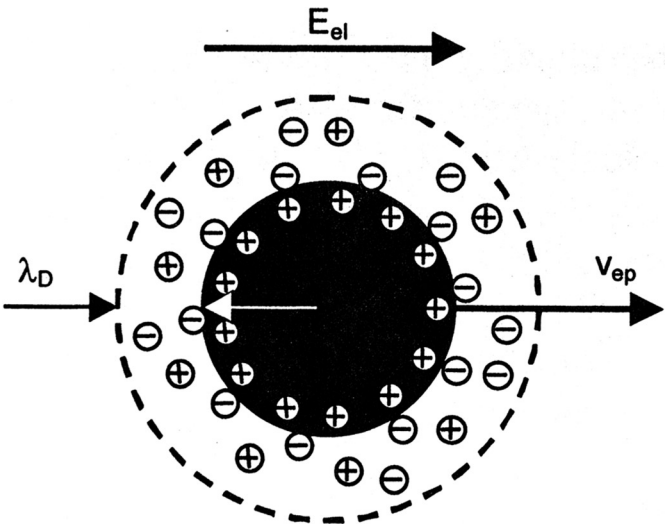

Figure 5.16 Charge distribution around an electrophoretic particle. [Reprinted with permission from Nguyen and Wereley (2002), copyright Artech House.]

A particle's electrophoretic velocity may be calculated by *the Smoluchowski equation* [Li, 2004]:

$$v_{ep} = -\frac{E_z \varepsilon_r \varepsilon_o \zeta_p}{\mu}, \tag{5.37}$$

where

v_{ep} is the particle's electrophoretic velocity,
E_z is the applied electrical field (V/m),
ε_r is the dielectric constant of the medium,
ε_o is the permittivity of a vacuum,
ζ_p is the zeta potential of the particle, and
μ is the viscosity.

Electrophoretic motility is defined as the electrophoretic velocity per unit of applied electrical field strength, characterizing how fast a particle moves in an electrical field:

$$v_E = \frac{v_{\text{ep}}}{E_z} = \frac{\varepsilon_r \varepsilon_o \zeta_p}{\mu}. \tag{5.38}$$

To be more precise it is necessary to consider frictional forces acting on the particle and *electrophoretic retardation.* Electro-osmosis in the EDL region of the particle causes reduction in the velocity, or retardation of the particles electrophoretic motion. Consider a negatively charged particle. Its electrophoretic motion will be toward the positive electrode, while the surrounding positive ions will be driven toward the negative electrode by electro-osmosis.

An underlying assumption in the Smoluchowski equation is that electroosmosis is the dominant force, and the particle's motion is equal to and opposite of the liquid motion.

A more general formulation for electrophoretic velocity is *Henry's equation*:

$$v_{ep} = \frac{2}{3}\frac{\varepsilon_r \varepsilon_o E_z \zeta_p}{\mu} f(\kappa a), \tag{5.39}$$

where

$f(\kappa a)$ is *Henry's function*.

Henry's function approaches 1 for small κa, and $3/2$ for large κa [Li, 2004].

5.3.3.2 Applications

Electrophoresis is most commonly done to separate molecules based on size. When performed in microchannels, the process is referred to as capillary electrophoresis. In genetic molecular diagnostics, electrophoresis is commonly preceded by PCR amplification of specific target nucleic acid sequences. This applies to DNA that may be endogenous to a patient's genome or exogenous, such as from bacteria or viruses. PCR is discussed in Chapter 11, *Genomics and DNA Microarrays*, and capillary electrophoresis (CE) is discussed in Chapter 9, *Micro-Total-Analysis Systems.*

Traditionally electrophoresis has been performed on agarose or polyacrylamide slab gel. Application of an electric field separates components based on their electrophoretic motility. Readout may occur by direct visualization after staining or by automated means. Agarose separation takes about 45 min, and polyacrylamide separation takes about 8 h (due to high resolution).

In his excellent review of molecular diagnostics on electrophoretic microchips, Landers (2003) emphasizes the importance of sample preparation and purification even prior to the PCR step, and that the electrophoretic separation itself is relatively minor to the entire process. This is important to bioMEMS designers to consider, and acts as a reminder that microfluidic devices are merely one component in a chain of devices that can be considered a μTAS.

5.3.4 Streaming potential

Forcing an aqueous-ion-containing solution through a microchannel under applied hydrostatic force induces a resistance to flow known as the *electroviscous effect.* As fluid is pushed through the channel, the counterions in the diffuse layer (the mobile part of the EDL) are also pushed along, creating a *streaming current.* A potential difference builds up along the channel wall known as the *streaming potential.* This streaming potential acts to drive the counterions in the diffuse layer in an opposite direction, generating an electrical current called the

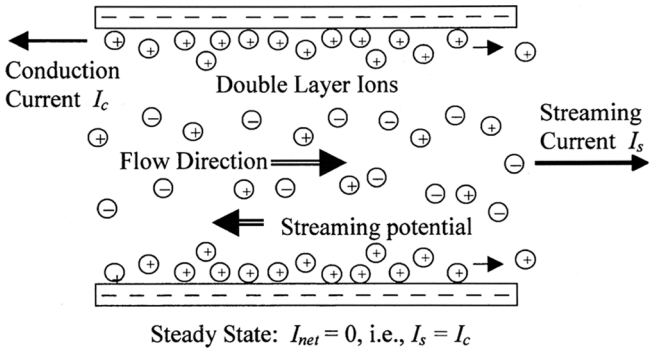

Figure 5.17 Illustration of the flow-induced electrokinetic field in a microchannel. [Reprinted with permission from Li (2004), copyright Elsevier.]

conduction current (Fig. 5.17). This drag on flow makes the fluid seem more viscous because the predicted flow is greater than what is actually observed [Ren and Li, 2004].

5.3.5 Dielectrophoresis

Dielectrophoresis is the physical phenomenon whereby dielectric particles, in response to a spatially nonuniform electric field, experience a net force directed toward locations with *increasing* or *decreasing* field intensity according to the physical properties of particles and medium. In the first case, the force is called *positive dielectrophoresis* (pDEP), while in the second case it is called *negative dielectrophoresis* (nDEP) [Medoro et al., 2003]. If the particle is charged, it also experiences a coulombic force superimposed on the dielectrophoretic force due to the nonuniform field.

Dielectrophoresis is proposed for cell and particle sorting, cell focusing, cell-ac-impedance analysis, cell lysis, and the manipulation of molecules and reagents droplets. Dielectrophoresis may also be used in nonmechanical pumping.

5.3.6 Electrowetting

As an alternative or complement to microfluidic channels, research has been performed on planar surfaces covered with electrodes that can be individually addressed (*digital microfluidics*) for the purpose of manipulating samples and reagents. All of the movement is confined between plates. Theoretically it is possible to create droplets from samples and reagents; divide, transport and merge them for purposes of dilution and reaction; isolate them for detection; and finally dispose of unwanted waste products.

Surface tension is a property of the liquid and is dependent on temperature and the other fluid it is in contact with. At the interface between a liquid and a gas, or

between two immiscible liquids, forces develop in the liquid surface that causes the surface to behave as if a "membrane" were stretched over it. This phenomenon is due to unbalanced cohesive forces acting on the liquid molecules at the fluid interface. Surface tension is the intensity of molecular attraction per unit length along any line in the surface [Young et al., 2001].

The phenomena of *electrowetting* and *electrocapillary* are that an externally added electrostatic charge modifies the surface tension or capillary forces at the fluid-surface interface. Figure 5.18 shows the influence of a charge on a droplet atop a planar electrode, and surrounded by a dielectric material. Cho et al. (2003) report on an electrowetting-on-dielectric (EWOD) device and have achieved cutting, merging, creating, and transporting of liquid droplets. Movement is achieved by asymmetrically changing the interfacial tension. An asymmetric deformation of the liquid meniscus occurs, which establishes a pressure difference inside the liquid and subsequent bulk fluid movement.

To understand these phenomena we need to first understand the concept of *wetting*. *Young's equation* (after Thomas Young who first proposed it in 1805)

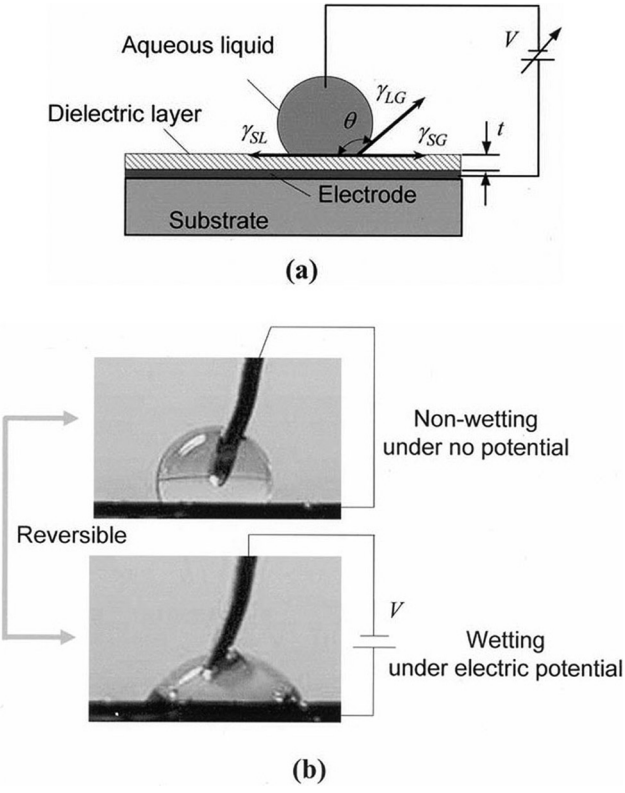

Figure 5.18 Principle of electrowetting on dielectric (EWOD): (a) schematic configuration; and (b) demonstration with ~5-μl fluid volume (see text for mathematical analysis). [Reprinted with permission from Cho et al. (2003), copyright IEEE.]

describes the simple balance of force between the liquid-solid, liquid-vapor, and solid-vapor interfacial surface energies of a droplet on a solid surface. The liquid-solid interfacial energy plus the component of the liquid-vapor interfacial energy that lies in the same direction must exactly balance the solid-vapor interfacial energy at equilibrium. At equilibrium, the *contact angle* θ is formed at the three-phase solid-liquid-gas junction. The contact angle may have values form 0 deg to 180 deg. At $\theta = 0$ deg, the liquid forms a thin layer on the surface. At $\theta = 180$ deg the entire droplet sits as a sphere on the surface (*nonwetting*) [Mitchell, 2004]:

$$\gamma_{LG} \cos \theta + \gamma_{SL} = \gamma_{SG}, \tag{5.40}$$

where

γ_{LG} is the liguid-gas interfacial tension,
γ_{SL} is the solid-liquid interfacial tension,
γ_{SG} is the solid-gas interfacial tension, and
θ is the contact angle.

The effect of a potential V on the contact angle is then determined by

$$\cos\theta\,(V) - \cos\theta_o = \frac{\varepsilon_r \varepsilon_o}{2\gamma_{LG} t} V^2, \tag{5.41}$$

where

θ is the contact angle,
θ_o is the equilibrium contact angle at $V = 0$,
V is the electric potential across the interface,
ε_r the dielectric constant of the dielectric layer,
ε_o is the permittivity of a vacuum (8.85×10^{-12} F/m), and
t is its thickness.

The envisioned digital microfluidic circuit and four fundamental droplet operations are shown in Fig. 5.19.

Fair et al. (2003) report the results of experiments on electrowetting for sample processing, on-chip preconcentration and dilution, on-chip sample injection or dispensing, and sample mixing. They have shown that high-speed transport and mixing of analytes and reagents can be performed using biological solutions without system contamination.

5.4 Microvalves

5.4.1 Introduction

As noted at the beginning of this chapter, microfluidic devices consist of channels, valves, mixers, pumps, filters, and heat exchangers to allow dilution, separation, mixing, and incubation of reaction materials and reagents. Both passive and active microvalves are available in the bioMEMS designer's toolbox.

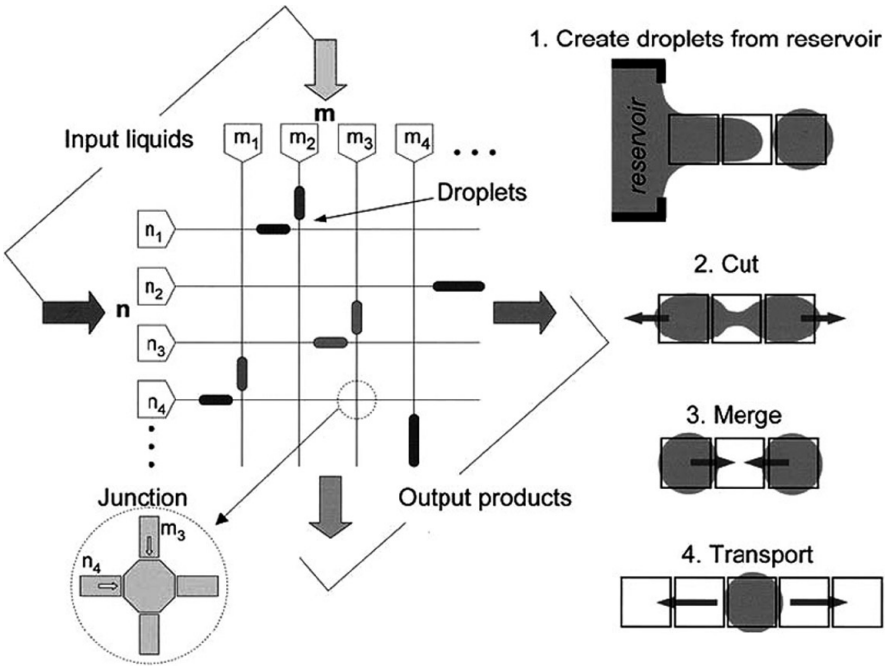

Figure 5.19 The envisioned digital microfluidic circuit and the four fundamental droplet operations necessary. [Reprinted with permission from Cho et al. (2003), copyright IEEE.]

5.4.2 Passive microvalves

Passive valves may be "check valves" that allow fluid to pass only in one direction, or they may be "stop" valves where their function is derived from hydrophobicity and immobilization of fluid. The former are often made from smart polymers that respond to environmental stimuli (pH, temperature, calcium, magnesium, fields, etc.). Hydrophobic regions may be created by surface modifications of a channel wall to create "virtual walls" that contain fluid.

Beebe et al. (2002) describe development of a biomimetic hydrogel check valve shown in Fig. 5.20. The valve leaflets are created by polymerization of pH sensitive hydrogel strips and anchors are then fabricated with non-pH sensitive strips. Basic solutions cause the hydrogel to expand and close the valve. Acidic solutions cause the hydrogel to contact and open the valve.

Passive hydrophobic valves are also discussed by Feng et al. (2003). Two naturally hydrophilic surfaces, silicon dioxide and Pyrex glass, were modified with octadecyltrichlorosilane (OTS) SAMs to make them hydrophobic. The "contact angle" of fluid drops on a surface defines its hydrophilicity/hydrophobicity, and is described below in the context of surface tension pumps. The fabricated stop valves were shown to stop flow of a liquid in both directions in a microchannel.

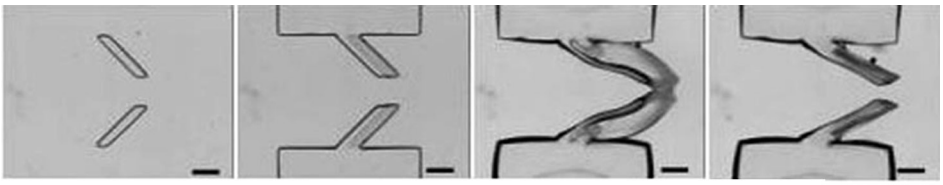

Figure 5.20 Hydrogel check valve. (a) Valve leaflets, (b) anchors, (c) expanding and closing the valve, and (d) contacting and opening the valve. [Reprinted with permission from Beebe et al. (2002), copyright Annual Reviews.]

5.4.3 Active microvalves

Active valves may be analog or digital, and have an initial state that is normally open, normally closed, or bistable (air, fluid, or electrical pulses alternate the state). An analog *proportional valve* has a flow that is a function of the valve opening. To accomplish this digitally there must be either a digital-to-analog conversion or the use of pulse-width modulation (i.e., rapid opening and closing).

Active valves include pneumatic, thermopneumatic, thermomechanical, piezoelectric, electrostatic, electromagnetic, electrochemical, and capillary force (electrocapillary and thermocapillary) [Nguyen and Wereley, 2002]. Some of these are discussed here.

Pneumatic valves require an external air source, and have response times of several hundred milliseconds to seconds. *Thermopneumatic valves* rely on changes in the volume of a hermetically sealed liquid or solid under thermal loading. They may also use a phase change from liquid to gas or from solid to liquid to gain a larger volume expansion. Kim et al. (2004) describe fabrication of a normally open thermopneumatic-actuated microvalve made from the PDMS and indium-tin-oxide (ITO) coated glass (as a heater element). Deflection of PDMS occurs and the flow rate decreases as power is applied to the ITO heater. *Thermomechanical valves* convert thermal energy to mechanical stress, either by solid-expansion, bimetallic materials or shape-memory alloys.

Piezoelectric valves are based on the piezoelectric effect exhibited by certain materials such as lead zirconate titanate (PTZ), polyvinylidene (PVDF), and zinc oxide (ZnO). A mechanical stress on the material generates an electrical charge, and an applied electric field generates a mechanical strain in the material. Small strain and high stresses are generated and are suitable for applications requiring high force and small displacement. The relationship between strain and electric field is described by the piezoelectric coefficients d_{31} and d_{33}:

$$\begin{aligned} \varphi_{\text{longitudinal}} &= \varphi_{\text{transverse}} = d_{31} E_{\text{el}} \\ \varphi_{\text{vertical}} &= d_{33} E_{\text{el}} \end{aligned} \tag{5.42}$$

Electrostatic valves are based on the attractive force between two oppositely charged plates:

$$F = \frac{1}{2}\varepsilon_r \varepsilon_o A \left(\frac{V}{d}\right)^2 \left(\frac{\varepsilon_i d}{\varepsilon_r d_i + \varepsilon_i d}\right)^2, \tag{5.43}$$

where

A is the overlapping plate area,
d is the distance between plates,
d_i is an insulator layer thickness,
V is the applied voltage,
ε_r is the relative dielectric coefficient of the medium,
ε_i is the relative dielectric coefficient of the insulator, and
ε_o is the permittivity of a vacuum.

Electromagnetic valves offer the advantage of large deflection and disadvantage of size, low efficiency, and heat generation. Magnetic materials include nickel, iron, and various alloys. Electromagnetic valves have solenoid actuators with an electrically driven coil to create a magnetic field, and a ferromagnetic core that moves inside the coil. The vertical force F of a magnetic field B in direction z acting on a magnet with a magnetization M_m, and volume V is given by

$$F = M_m \int \frac{dB}{dz} dV, \tag{5.44}$$

where

M_m is the magnetization,
V the volume of the magnet,
B is the magnetic field, and
z is the direction in which the force is acting.

Capillary-force valves are based on active and passive control of surface tension and capillary forces. The *electrocapillary* valves use electrowetting phenomena to move fluid in a capillary. Recall the EDL charge distribution at the interface of the fluid a channel surface, where the negatively charged wall attracts positive charges in the fluid. If a dc potential is applied at either end of the capillary, the fluid moves toward the cathode (negative) end, and away from the anode end. *Thermocapillary* valves are based on the temperature dependence of surface tension, as shown in Fig. 5.21. At higher temperatures, the molecules of the liquid move faster and their attractive force become smaller. The smaller attractive force causes *lower viscosity and lower surface tension.* Movement towards the warmer end of the capillary occurs (opposite the intuitive direction).

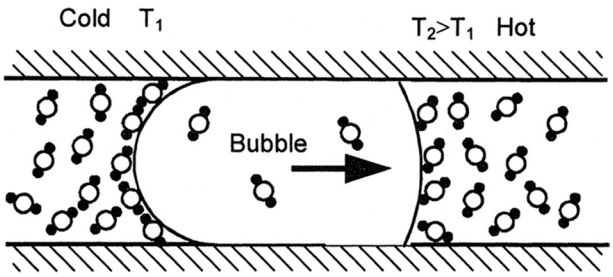

Figure 5.21 Thermocapillary effect, also called the Marangoni effect. [Reprinted with permission from Nguyen and Wereley (2002), copyright Artech House.]

5.4.4 Valve parameters

Important parameters by which valves are specified include leakage, valve capacity, power consumption, closing force (pressure range), temperature range, response time, reliability, biocompatibility, and chemical compatibility [Nguyen and Wereley, 2002]. A few of these are discussed below.

Leakage is the amount of flow through a normally closed valve. The leakage ratio is the flow of the valve in the closed state to that in the open state (ideally zero):

$$L_{\text{valve}} = \frac{\dot{Q}_{\text{closed}}}{\dot{Q}_{\text{open}}}, \tag{5.45}$$

where

$\dot{Q}_{\text{closed}}$ = flow rate in the closed position
$\dot{Q}_{\text{open}}$ = flow rate in the open position at a constant inlet pressure.

Valve capacity is the maximum flow rate:

$$C_{\text{Valve}} = \frac{\dot{Q}_{\max}}{\sqrt{\frac{\Delta p_{\max}}{\rho g}}}, \tag{5.46}$$

where

$\dot{Q}_{\max}$ is the flow rate across valve fully open,
$\Delta p_{\max}$ is the pressure drop across the valve fully open,
ρ is the fluid density, and
g is the acceleration of gravity.

Power consumption is the total input power of the valve in its active, power consuming state.

5.5 Micromixers

At the microscale, mixing in laminar flow occurs by diffusion as described above. Some assays require more rapid mixing, and this may be accomplished passively by channel geometry (see Fig. 5.22) or with active mixers.

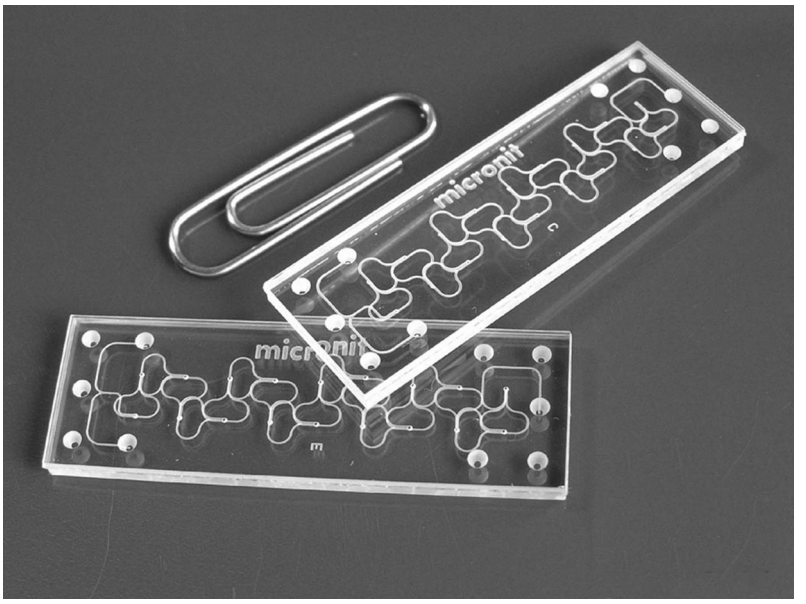

Figure 5.22 Micromixers. (Photo courtesy of Micronit, Inc.)

5.5.1 Passive and active mixers

Passive mixers rely on diffusion, and have no moving parts. Lamination mixing may be achieved with *T-mixers* and *Y-mixers*, and may be aided by using sequential plugs or a narrow orifice to cause turbulent flow (Fig. 5.23). *Chaotic advection* can be achieved by using serpentine geometries (Fig. 5.24) [Nguyen and Wereley, 2002]. *Injection mixers* split one stream into two or more substreams and then recombine them into a single stream.

The influence of surface heterogenicities on electro-osmotic flow has been studied by Erickson and Li (2003). They have shown that introduction of oppositely charged surface heterogeneities to the microchannel walls can result in regions of localized circulation within the bulk flow.

Active mixing increases the interfacial area between fluids and can be accomplished by piezoelectric devices, electrokinetic mixers, chaotic convection, and other pumping techniques below.

5.6 Micropumps

5.6.1 Introduction

LOC devices and μTAS often require some means of moving around samples and reagents, and both nonmechanical and mechanical means may be used. Micropumps also have a role in drug-delivery systems and are reviewed further in Chapter 7, *Microactuators and Drug Delivery.*

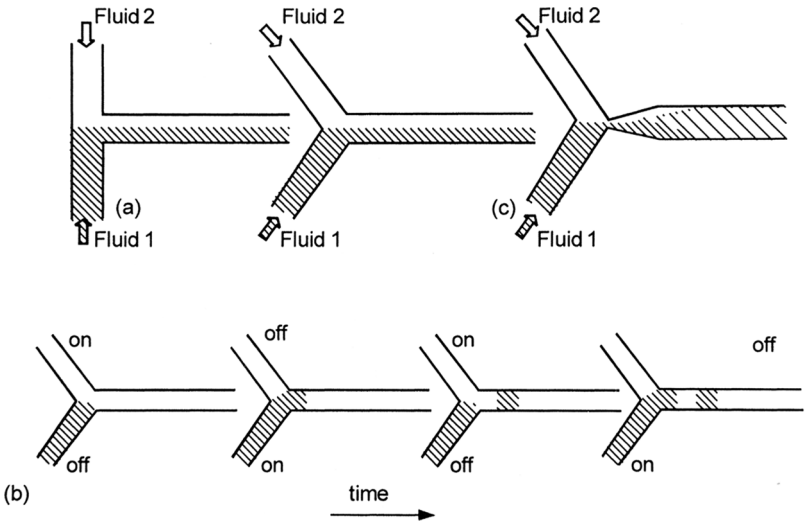

Figure 5.23 Passive mixers. (a) T-mixer and Y-mixer; (b) sequential mixing; and (c) a throttle design. [Reprinted with permission from Nguyen and Wereley (2002), copyright Artech House.]

5.6.2 Nonmechanical pumping

Electrokinetic pumping methods based on electro-osmosis, electrophoresis and dielectrophoresis have been discussed above. Precise low flow rates may be obtained as well as overcoming high circuit impedance. Pumping may also be

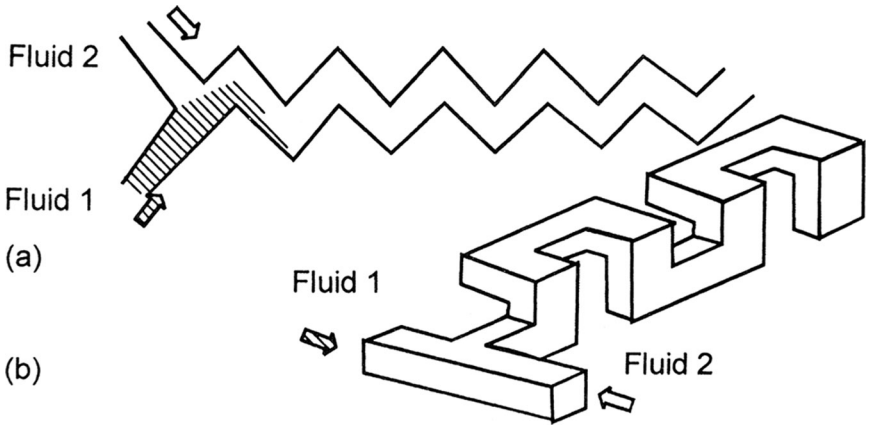

Figure 5.24 Serpentine mixers. (a) The planar serpentine structure has been found not to work in micromixers because of laminar flow in microscale [Branebjerg et al., 1994]; whereas (b) the 3D serpentine structure does provide chaotic advection to laminar flow. [Reprinted with permission from Liu et al. (1999), copyright IEEE.]

accomplished by taking advantage of surface tension and *capillary effects.* Surface tension effects are dominant over inertial effects at the microscale, and are fundamental to the operation of many microfluidic devices.

Figure 5.25 shows capillary-force-driven pumps for a hydrophilic surface, where the *contact angle* is between 0 deg and 90 deg and a hydrophobic surface capillary tube, where the contact angle will be between 90 deg to 180 (recall discussion of *Young's equation*).

In the hydrophilic case, the solid-liquid interface has a lower surface energy than the solid-gas interface, and the liquid column moves in the direction of the gas interface to minimize its surface energy. The energy balance in the liquid column and driving pressure are calculated as

$$2\pi r_o h(\gamma_{SG} - \gamma_{SL}) = \Delta p \pi r_o^2 h \quad \text{and} \quad \Delta p = \frac{2\gamma_{LG}\cos\theta}{r_o}, \tag{5.47}$$

where

r_o is the capillary radius,
h is the height of the column, and
Δp is the pressure difference across the gas-liquid interface.

Specified in more familiar terms of *surface tension* and *specific weight* the height is determined as follows:

$$h = \frac{2\sigma\cos\theta}{\gamma r_o}, \tag{5.48}$$

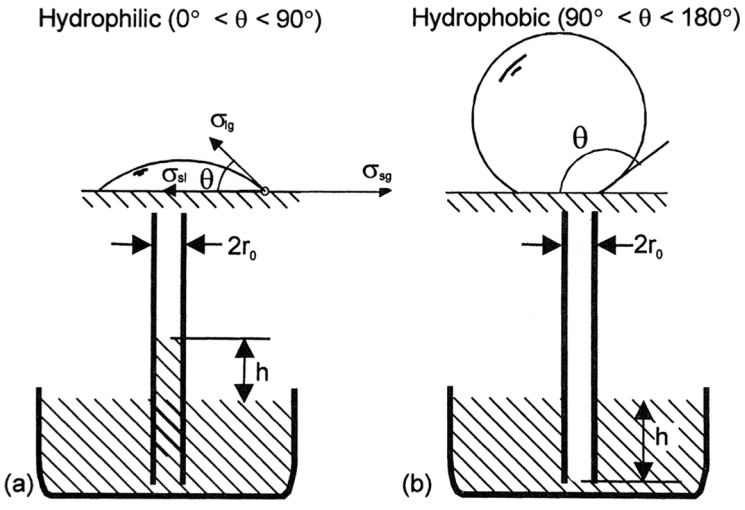

Figure 5.25 Capillary force driven pump: (a) hydrophilic; and (b) hydrophobic. [Reprinted with permission from Nguyen and Wereley (2002), copyright Artech House.]

where

σ is the surface tension (the same as γ_{LG} in N/m), and
γ is specific weight of the fluid (N/m^3).

The height is inversely related to the tube radius. When microchannels with dimensions on the order of microns are used, the lengths liquids travel based on capillary forces alone are significant.

5.6.3 Mechanical pumps

Micropumps may be classified as displacement pumps or dynamic pumps. In displacement pumps energy is periodically added to increase pressure to the point of overcoming channel and valve resistance. Dynamic pumps add mechanical energy continuously.

There are a variety of pump types, including "check valve" pumps, peristaltic pumps, valveless-rectification pumps, rotary pumps, centrifugal pumps, ultrasonic pumps, and magnetic pumps [Nguyen and Wereley, 2002].

Check-valve pumps consist of an actuator unit, a pump membrane that creates a stroke volume (displacement), a pump chamber with a dead volume (from which the stroke volume is delivered), and two passive check valves, which open when a critical pressure difference occurs. This is analogous to the human heart. Contracting smooth muscle of the heart serves as the actuator; while the mitral, pulmonary artery, tricuspid, and aortic valves function as check valves. Blood is pushed ahead, but does not move backwards (ordinarily) through the valves. Small check valves in the extremity veins also serve to augment blood flow when veins are periodically compressed by arm and leg movement. *Stroke volume* refers to the volume of blood ejected with each heart beat. There are numerous other *indices* of cardiac function that define this complex system.

Peristaltic pumps are based on the peristaltic motion of the pump chambers. While this may be accomplished by sequenced compression of multiple flexible chambers, a more physiological method would be to emulate the smooth muscle peristaltic contractile waves of the esophagus, stomach, and bowel.

Rotary pumps typically require external actuators, and may move fluid along by a turnstile mechanism (like automatic revolving doors) or by external compression (roller pumps) on flexible membranes (such as seen in intravenous pumps, feeding pumps, and extracorporal circulation pumps). *Centrifugal pumps* are based on the forces created by spinning a disk.

Ultrasonic pumps work by causing acoustic streaming, which is induced by a mechanical traveling wave. The mechanical wave can be either a flexural plate wave (FPW) or a surface acoustic wave (SAW). The mechanical wave is excited by interdigital transducers (IDT) placed on a thin membrane coated with piezoelectric film or on a piezoelectric bulk material. Piezoelectricity and SAWs are discussed in Chapter 6, *Sensor Principles and Microsensors.* Figure 5.26 shows a SAW device with superimposed grid to visualize the surface deformation due to wave propagation. The material points at the surface exhibit elliptical motion.

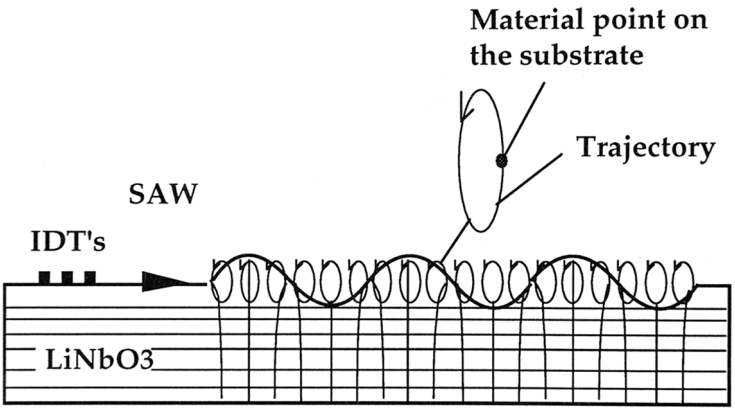

Figure 5.26 A surface acoustic wave or delay line showing surface deformation due to wave propagation. [Reprinted with permission from Tabib-Azar (1997), copyright Springer.]

Magnetic pumping uses magnetic fields to assist in pumping. Hartshorne et al. (2004) describe a magnetically driven system. Microfluidic valves and pumps were fabricated from etched glass substrates each bonded to a second glass substrate lid that had ultrasonically drilled access holes. The devices contained "ferrofluid plugs" approximately 10 mm in length that could be actuated by external magnets. The ferrofluid used in the devices was a colloidal suspension of ferromagnetic particles in a hydrophobic fluorocarbon carrier and was immiscible in water. Hartshorne found that coating channels with hydrophobic organ-saline prevented leakage of water around the ferrofluid plugs.

5.6.4 Pump parameters

Important pump parameters include maximum flow rate, maximum back pressure, pump head, and efficiency.

Maximum flow rate is the volume of liquid per unit of time delivered by the pump at zero back pressure ($Q_{\max}$). *Maximum back pressure* is the maximum pressure the pump can work against. At this pressure the flow rate becomes zero.

The *Bernoulli equation* shows that the total pressure (static, hydrostatic, and dynamic) remains constant along a streamline (for steady, inviscid, and incompressible flow):

$$p_{\text{Total}} = p + \frac{\rho V^2}{2} + \gamma z = \text{ constant along a streamline} \tag{5.49}$$

An equivalent form of this equation is to divide each term by the *specific weight.* Each of the terms of this equation has the *units of length* (or *energy per unit weight*)

and represents a certain type of *head*:

$$\frac{p}{\gamma}+\frac{V^2}{2g}+z=\text{constant along a streamline} \tag{5.50}$$

where

p/γ is the pressure head,
$V^2/2g$ is the velocity head, and
z is the elevation head.

The *extended Bernoulli equation* may be used to describe the energy equation for a 1D incompressible steady flow between two sections, such as an inlet and outlet. This is derived by dividing each term by the fluid density, adding a factor for *work per unit mass* performed by an actuator (such as a pump or turbine) and subtracting a *loss factor* for friction (inclusive of viscosity):

$$\frac{p_{\text{out}}}{\rho}+\frac{V_{\text{out}}^2}{2}+gz_{\text{out}}=\frac{p_{\text{in}}}{\rho}+\frac{V_{\text{in}}^2}{2}+gz_{\text{in}}+w_{\text{actuator}}-\text{loss}_{\text{friction}}. \tag{5.51}$$

Dividing by g puts the relationship in terms of energy per unit weight or head:

$$\frac{p_{\text{out}}}{\gamma}+\frac{V_{\text{out}}^2}{2g}+z_{\text{out}}=\frac{p_{\text{in}}}{\gamma}+\frac{V_{\text{in}}^2}{2g}+z_{\text{in}}+h_s-h_L, \tag{5.52}$$

where h_s is defined as

$$\begin{aligned} h_s &= \frac{w_{\text{actuator}}}{g}=\frac{\dot{W}_{\text{actuator}}}{\dot{m}g} \text{ (or work per unit mass of the actuator)} \\ &= \frac{\dot{W}_{\text{actuator}}}{\gamma Q}, \end{aligned} \tag{5.53}$$

where

$\dot{W}_{\text{actuator}}$ is the power delivered to the actuator,
$\dot{m}$ is the mass flowrate $=\rho AV=\rho Q$,
V is the component of fluid velocity normal to the area A, and
Q is the volume flow rate.

For a pump in control volume, the *pump head* equals h_s and the *head loss* is h_L. The *efficiency* is the ratio of amount or work that produces a useful effect [Young et al., 2001]:

$$\eta=\frac{w_{\text{actuator}}-\text{loss}}{w_{\text{actuator}}} \quad \text{and} \quad w_{\text{actuator}}=\frac{\dot{W}_{\text{actuator}}}{\dot{m}}. \tag{5.54}$$

5.7 Review Questions

1. What opportunities do microfluidic devices offer?
2. List several of the components of a microfluidic device.

3. What are the advantages and disadvantages of materials used for microfluidic devices (including glass, quartz, silicon, and polymers)?
4. Describe methods for fabricating channels in silicon and polymers, including surface micromachining.
5. How are parylene materials useful for bioMEMS devices?
6. What is the difference between the Eulerian and Lagrangian methods in analyzing fluid mechanics problems?
7. What is the relationship between a sample volume and analyte concentration?
8. Define a fluid generally and a Newtonian fluid. Define viscosity, kinematic viscosity, specific weight, and specific gravity.
9. Describe fully what is meant by a field representation of flow and streamlines.
10. Describe Hagen-Poiseuille flow and Poiseuille's law.
11. Define surface area to volume and its importance for microfluidic devices.
12. Why is diffusion important in microfluidic devices? How is it calculated?
13. Define electro-osmosis, EOF, and the Poisson equation.
14. Show the Boltzmann equation, including a description of each term, and explains its usefulness. Show the Poisson-Boltzmann equation and the more general form of the equation that considers charge density.
15. Show calculation of the Debye-Huckel parameter and describe what it represents. Derive the equation for the characteristic thickness of the EDL based on the molarity of the solution.
16. Write the Poisson-Boltzmann equation in terms of the Debye-Huckel parameter and of a nondimensional electric potential.
17. Describe the orgin of surface charge on various materials.
18. Explain the EDL and show the calculation of the distribution of ions near a charged surface.
19. Show the calculation of EOF for a simple slit channel.
20. Define electrophoresis and show the calculation of a particle's electrophoretic velocity and electrophoretic motility.
21. Define streaming potential and dielectrophoresis.
22. Describe electrowetting and electrocapillary. Include a discussion of Young's equation and calculation of the contact angle in the presence of an electric potential.
23. What is the difference between active and passive microvalves? Describe how electrostatic valves work, showing calculation of the attractive force.
24. Describe the energy balance in a liquid column, and calculate the height fluid rising in a capillary tube. How will the contact angle vary between hydrophobic and hydrophilic surfaces?
25. Show the derivation of pump efficiency and pump head using the Bernoulli equation and the extended Bernoulli equation.

References

Beebe, D.J., G.A. Mensing, and G.M. Walker, "Physics and applications of microfluidics in biology." *Annual Review of Biomedical Engineering* 4, pp. 261–286 (2002).

Bottausci, F., I. Mezic, C.D. Meinhart, and C. Cardonne, "Mixing in the shear superposition micromixer: three-dimensional analysis." *Philosophical Transactions of the Royal Society of London Series A—Mathematical Physical and Engineering Sciences* 362(1818), pp. 1001–1018 (2004).

Bousse, L. et al., "Electrokinetically controlled microfluidic analysis systems." *Annual Review of Biophysics and Biomolecular Structure* 29, pp. 155–181 (2000).

Branebjerg, J. et al., "Application of miniature analyzers from microfluidic components to microTAS." *Proceedings of Micro-total-analysis systems Conference*, pp. 141–151 (1994).

Cho, S.K., H.J. Moon, and C.J. Kim, "Creating, transporting, cutting, and merging liquid droplets by electrowetting-based actuation for digital microfluidic circuits." *Journal of Microelectromechanical Systems* 12(1), pp. 70–80 (2003).

Debesset, S. et al., "An AC electrokinetic micropump for circular chromatographic applications." *Lab Chip* 4, pp. 396–400 (2004).

Erickson, D. and D. Li, "Three-dimensional structure of electro-osmotic flow over heterogeneous surfaces." *Journal of Physical Chemistry B* 107(44), pp. 12212–12220 (2003).

Fair, R.B. et al., "Electrowetting-based on-chip sample processing for integrated microfluidics." *Proceedings of IEEE International Electron Devices Meeting*, pp. 779–782 (2003).

Feng, Y., Z. Zhou, X. Ye, and J. Xiong, "Passive valves based on hydrophobic microfluidics." *Sensors and Actuators, A: Physical* 108(1:3), pp. 138–143 (2003).

Hartshorne, H., C.J. Backhouse, and W.E. Lee, "Ferrofluid-based microchip pump and valve." *Sensors and Actuators, B: Chemical* 99(2:3), pp. 592–600 (2004).

Kim, J.-H. et al., "A disposable thermopneumatic-actuated microvalve stacked with PDMS layers and ITO-coated glass." *Proceedings of Micro and Nano Engineering* 73–74, pp. 864–869 (2004).

Kuricheti, K.K., V. Buschmann, P. Brister, and K.D. Weston, "Velocity imaging in microfluidic devices using fluorescence correlation spectroscopy." *Proceedings of SPIE* 5345, pp. 194–205 (2004).

Landers, J.P., "Molecular diagnostics on electrophoretic microchips." *Analytical Chemistry* 75(12), pp. 2919–2927 (2003).

Li, D., *Electrokinetics in Microfluidics, 1st ed., Vol. 2.*, Elsevier, Amsterdam (2004).

Liu, R.H. et al., "A passive micromixer: three-dimensional serpintine microchannel." *Proceedings of Transducer '99*, pp. 730–733 (1999).

Liu, X., D. Erickson, D. Li, and U.J. Krull, "Cationic polymer coatings for design of electro-osmotic flow and control of DNA adsorption." *Analytica Chimica Acta* 507(1), pp. 55–62 (2004).

Manz, A., N. Graber, and H.M. Widmer, "Miniaturized total chemical analysis systems, a novel concept for chemical sensing." *Sensors and Actuators, B: Chemical* B1(1:6), pp. 244–248 (1990).

Manz, A., "Miniaturized chemical analysis systems based on electro-osmotic flow." *Proceedings of the International Workshop on Micro Electro Mechanical Systems*, pp. 14–18 (1997).

Medoro, G. et al., "A lab-on-a-chip for cell detection and manipulation." *IEEE Sensors Journal* 3(3), pp. 317–325 (2003).

Mitchell, B.S., *An Introduction to Materials Engineering and Science for Chemical and Materials Engineers.* Wiley, Hoboken, NJ (2004).

Munson, B.R., D.F. Young, and T.H. Okiishi, *Fundamentals of Fluid Mechanics, 4th ed.*, Wiley, New York (2002).

Nguyen, N.-T. and S.T. Wereley, *Fundamentals and Applications of Microfluidics.* Artech House, Boston, MA (2002).

Peterson, K.E. et al., "Toward next generation clinical diagnostics instruments: scaling and new processing paradigms." *Journal of Biomedical Microdevices* 2(1), pp. 71–79 (1999).

Peng, X.F., G.P. Peterson, and B.X. Wang, "Frictionless flow characteristics of water flowing through rectangular microchannels." *Experimental Heat Transfer* 7(4), pp. 249–264 (1994).

Qiao, R. and N.R. Aluru, "Atypical dependence of electro-osmotic transport on surface charge in a single-wall carbon nanotube." *Nano Letters* 3(8), pp. 1013–1017 (2003).

Ren, L. et al., "Electro-osmotic flow in a microcapillary with one solution displacing another solution." *Journal of Colloid and Interface Science* 242, pp. 264–271 (2001).

Ren, C.L. and D. Li., "Electroviscous effects on pressure-driven flow of dilute electrolyte solutions in small microchannels." *Journal of Colloid and Interface Science* 274(1), pp. 319–330 (2004).

Stay, M.S. and V.H. Barocas, "Thin-domain modeling of mass transport in microchannels, with applications to diffusive mixing." *Journal of Applied Physics* 95(11I), pp. 6435–6443.

System Planning Corporation, *Microelectromechanical Systems (MEMS): An SPC Market Study.* Arlington, VA (1999).

Szumski, M. and B. Buszewski, "State of the art in miniaturized separation techniques." *Critical Reviews in Analytical Chemistry* 32(1), pp. 1–46 (2002).

Tabib-Azar, M., *Microactuators: Electrical, Magnetic, Thermal, Optical, Mechanical, Chemical, and Smart Structures.* Kluwer Academic, Boston (1997).

Tang, G.Y., C. Yang, C.J. Chai, and H.Q. Gong, "Modeling of electro-osmotic flow and capillary electrophoresis with the joule heating effect: the Nernst-Planck equation versus the Boltzmann distribution." *Langmuir* 19(26), pp. 10975–10984 (2003).

Tay, F.E.H., *Microfluidics and BioMEMS Applications, Vol. 10.* Kluwer Academic Publishers, Boston (2002).
Verpoorte, E. and N.F. De Rooij, "Microfluidics meets MEMS." *Proceedings of the IEEE* 91(6), pp. 930–953 (2003).
Verpoorte, E. et al., "A novel optical detector cell for use in miniaturized total chemical analysis systems." *International Conference on Solid-State Sensors and Actuators*, pp. 796–799 (1991).
Verpoorte, E. et al., "Silicon flow cell for optical detection in miniaturized total chemical analysis systems." *Sensors and Actuators, B: Chemical* B6(1–3), pp. 66–70 (1992).
Young, D.F., B.R. Munson, and T.H. Okiishi, *A Brief Introduction to Fluid Mechanic, 2nd ed.*, Wiley, New York (2001).

Suggested Reading

Electro-osmotic flow in rectangular microchannels

Arulanandam, S. and D. Li, "Liquid transport in rectangular microchannels by electro-osmotic pumping." *Colloids and Surfaces A: Physicochemical and Engineering Aspects* 161(1), pp. 89–102 (2000).
Yang, C. and D. Li, "Analysis of electrokinetic effects on the liquid flow in rectangular microchannels." *Colloids and Surfaces A: Physicochemical and Engineering Aspects* 143(2:3), pp. 339–353 (1998).

Electrowetting

Ding, H., K. Chakrabarty, and R.B. Fair, "Scheduling of microfluidic operations for reconfigurable two-dimensional electrowetting arrays." *IEEE Transactions on Computer-Aided Design of Integrated Circuits and Systems* 20(12), pp. 1463–1468 (2001).
Moon, H., S.K. Cho, R.L. Garrell, and C.J. Kim, "Low voltage electrowetting-on-dielectric." *Journal of Applied Physics* 92(7), pp. 4080–4087 (2002).
Paik, P., V.K. Pamula, M.G. Pollack, and R.B. Fair, "Electrowetting-based droplet mixers for microfluidic systems." *Lab on a Chip* 3(1), pp. 28–33 (2003).
Pollack, M.G., A.D. Shenderov, and R.B. Fair, "Electrowetting-based actuation of droplets for integrated microfluidics." *Lab on a Chip* 2(2), pp. 96–101 (2002).
Torkkeli, A., "Droplets microfluidics on a planar surface." *VTT Publications* 504, pp. 1–194 (2003).

Passive micromixers

Bessoth, F.G., A.J. deMello, and A. Manz, "Microstructure for efficient continuous flow mixing." *Analytical Communications* 36(6), pp. 213–215 (1999).

Biddiss, E., D. Erickson, and D. Li, "Heterogeneous surface charge enhanced micromixing for electrokinetic flows." *Analytical Chemistry* 76(11), pp. 3208–3213 (2004).

Hardt, S. and F. Schonfeld, "Laminar mixing in different interdigital micromixers, II. Numerical simulations." *AICHE Journal* 49(3), pp. 578–584 (2003).

Haverkamp, V. et al., "The potential of micromixers for contacting of disperse liquid phases." *Fresenius Journal of Analytical Chemistry* 364(7), pp. 617–624 (1999).

Hessel, V., S. Hardt, H. Lowe, and F. Schonfeld, "Laminar mixing in different interdigital micromixers, I. Experimental characterization." *AICHE Journal* 49(3), pp. 566–577 (2003).

Hong, C.C., J.W. Choi, and C.H. Ahn, "A novel in-plane passive microfluidic mixer with modified Tesla structures." *Lab on a Chip* 4(2), pp. 109–113 (2004).

Jen, C.P., C.Y. Wu, and Y.C. Lin, "Design and simulation of the micromixer with chaotic advection in twisted microchannels." *Lab on a Chip* 3(2), pp. 77–81 (2003).

Kakuta, A., F.G. Bessoth, and A. Manz, "Microfabricated devices for fluid mixing and their application for chemical synthesis." *Chemical Record: An Official Publication of the Chemical Society of Japan* 1(5), pp. 395–405 (2001).

Kim, D.S., S.W. Lee, T.H. Kwon, and S.S. Lee, "A barrier embedded chaotic micromixer." *Journal of Micromechanics and Microengineering* 14(6), pp. 798–805 (2004).

Koch, M., H. Witt, A.G.R. Evans, and A. Brunnschweiler, "Improved characterization technique for micromixers." *Journal of Micromechanics and Microengineering* 9(2), pp. 156–158 (1999).

Melin, J. et al., "A fast passive and planar liquid sample micromixer." *Lab on a Chip* 4(3), pp. 214–219 (2004).

Park, S.J. et al., "Rapid three-dimensional passive rotation micromixer using the breakup process." *Journal of Micromechanics and Microengineering* 14(1), pp. 6–14 (2004).

Vijayendran, R.A., K.M. Motsegood, D.J. Beebe, and D.E. Leckband. "Evaluation of a three-dimensional micromixer in a surface-based biosensor." *Langmuir* 19(5), pp. 1824–1828 (2003).

Wang, H., P. Iovenitti, E. Harvey, and S. Masood "Passive mixing in micro-channels by applying geometric variations." *Proceedings of SPIE* 4982, pp. 282–289 (2003).

Wong, S.H., M.C.L. Ward, and C.W. Wharton, "Micro t-mixer as a rapid mixing micromixer." *Sensors and Actuators B-Chemical* 100(3), pp. 359–379 (2004).

Active micromixers

Biddiss, E., D. Erickson, and D. Li, "Heterogeneous surface charge enhanced micromixing for electrokinetic flows." *Analytical Chemistry* 76(11), pp. 3208–3213 (2004).

Erickson, D. and D. Li, "Influence of surface heterogeneity on electrokinetically driven microfluidic mixing." *Langmuir* 18(5), pp. 1883–1892 (2002).

Lastochkin, D. et al., "Electrokinetic micropump and micromixer design based on ac faradaic polarization." *Journal of Applied Physics* 96(3), pp. 1730–1733 (2004).

Liu, R.H., R. Lenigk, and P. Grodzinski, "Acoustic micromixer for enhancement of DNA biochip systems." *Journal of Microlithography, Microfabrication, and Microsystems* 2(3), pp. 178–184 (2003).

Lu, L.H., K.S. Ryu, and C. Liu, "A magnetic microstirrer and array for microfluidic mixing." *Journal of Microelectromechanical Systems* 11(5), pp. 462–469 (2002).

Tabeling, P. et al., "Chaotic mixing in cross-channel micromixers." *Philosophical Transactions of the Royal Society of London Series A-Mathematical Physical and Engineering Sciences* 362(1818), pp. 987–1000 (2004).

Yang, Z., H. Goto, M. Matsumoto, and R. Maeda, "Active micromixer for microfluidic systems using lead-zirconate-titanate(PZT)-generated ultrasonic vibration." *Electrophoresis* 21(1), pp. 116–119 (2000).

Yang, Z. et al., "Ultrasonic micromixer for microfluidic systems." *Sensors and Actuators A-Physical* 93(3), pp. 266–272 (2001).

Micropumps

Ahn, C.H. and M.G. Allen. "Fluid micropumps based on rotary magnetic actuators." *Proceedings of IEEE Micro Electro Mechanical Systems Conference*, pp. 408–412 (1995).

Arulanandam, S. and D. Li, "Liquid transport in rectangular microchannels by electro-osmotic pumping." *Colloids and Surfaces A: Physicochemical and Engineering Aspects* 161(1), pp. 89–102 (2000).

Benard, W.L., H. Kahn, A.H. Heuer, and M.A. Huff, "Thin-film shape-memory alloy actuated micropumps." *Journal of Microelectromechanical Systems* 7(2), pp. 245–251 (1998).

Chang, W.J. et al., "Pneumatically bidirectional microfluidic regulation using venturi pumps by deep RIE and bonding technology." *Microsystem Technologies* 8(4:5), pp. 318–322 (2002).

Darabi, J. and H. Wang, "Opportunities and challenges in micropump technology." *Proceedings of ASME International Mechanical Engineering Congress and Exposition* 7, pp. 21–28 (2002).

Huang, L., W. Wang, and M.C. Murphy, "Lumped-parameter model for a micropumps based on the magnetohydrodynamic (MHD) principle." *Proceedings of SPIE* 3680, pp. 379–387 (1999).

Ikuta, K., A. Takahashi, K. Ikeda, and S. Maruo, "Fully integrated micro biochemical laboratory using biochemical IC chips—cell-free protein synthesis by using a built-in micropump chip." *Proceedings of IEEE Micro Electro Mechanical Systems*, pp. 451–454 (2003).

Lee, D.E., H.-P. Chen, S. Soper, and W. Wang, "An electrochemical micropump and its application in a DNA mixing and analysis system." *Proceedings of SPIE* 4982, pp. 264–271 (2003).

Na, S., S. Ridgeway, and L. Cao, "Theoretical and experimental study of fluid behavior of a peristaltic micropump." *15th Biennial Microelectronics Symposium*, pp. 312–316 (2003).

Olsson, A. et al., "Valve-less diffuser micropumps fabricated using thermoplastic replication." *Sensors and Actuators, A: Physical*, 64(1), pp. 63–68 (1998).

Pan, T. et al., "A magnetically driven PDMS peristaltic micropump." *Proceedings of the IEEE Engineering in Medicine and Biology Society*, pp. 2639–2642 (2004).

Reichmuth, D.S., G.S. Chirica, and B.J. Kirby, "Increasing the performance of high-pressure, high-efficiency electrokinetic micropumps using zwitterionic solute additives." *Sensors and Actuators, B: Chemical* 92(1:2), pp. 37–43 (2003).

Schomburg, W.K. et al., "Microfluidic components in LIGA technique." *Journal of Micromechanics and Microengineering* 4(4), pp. 186–191 (1994).

Smits, J.G. "Piezoelectric micropump with three valves working peristaltically." *Sensors and Actuators, A: Physical* 21(1:3), pp. 203–206 (1990).

Soerensen, O., K.S. Drese, W. Ehrfeld, and H.-J. Hartmann, "Micromachined flow handling component—micropumps." *Proceedings of SPIE* 3857, pp. 52–60 (1999).

Takamura, Y. et al., "Low-voltage electro-osmosis pump for stand-alone microfluidics devices." *Electrophoresis* 24(1:2), pp. 185–192 (2003).

Varadan, V.K. and V.V. Varadan, "Micro pump and venous valve by micro stereo lithography." *Proceedings of SPIE* 3990, pp. 246–254 (2000).

Watler, P.K. and M.V. Sefton, "Piezoelectric driven controlled release micropump for insulin delivery." *ASAIO (American Society for Artificial Internal Organs) Transactions* 36(2), pp. 70–77 (1990).

Xu, B. et al., "Design and development of application specific microfluidic components for flow control." *Proceedings of SPIE* 4982, pp. 256–263 (2003).

Acronyms

μCAE	Microcapillary electrophoresis
μCP	Microcontact printing
μTAS	Micro-total-analysis systems
μTM	Microtransfer molding
3D-CSP	Three-dimensional chip scale packaging
AA	Acrylic acid
AAm	Acylamide
ABET	Accreditation Board for Engineering and Technology
ABS	Poly(acrylonitrile-co-butadiene-co-styrene)
ac	Alternating current
AFM	Atomic force microscopy
AIChe	American Institute of Chemical Engineers
AMANDA	Surface micromachining, micromolding, and diaphragm transfer
APTS	Aminopropyltrimethoxysilane
ARL	Army Research Laboratory
ASIC	Application specific integrated circuit
ASME	American Society of Mechanical Engineers
ASR	Analyte specific reagents
ASTM	The American Society for Testing and Materials
AT-PMMA	Amine terminated PMMA
BCC	Body-centered cubic
BioFET	Biologically active FET
BioMEMS	Biomedical microelectromechanical systems
BL	Bioluminescence
BMES	Biomedical Engineering Society
Bq	Becquerel
CAD	Computer-aided design
CAE	Capillary array electrophoresis
CAIBE	Chemical assisted ion beam etching
CCD	Charge-coupled device
cDNA	Complimentary DNA
CDRH	Center for Devices and Radiological Health
CE	Capillary electrophoresis
CEA	Carcinoembryonic antigen

CFR	Code of Federal Regulation
Ci	Curie
CL	Chemiluminescence
CLFS	Clinical laboratory fee schedule
CLIA	Clinical Laboratories Improvement Act
CMD	Carboxymethylated dextran
CMOS	Complementary metal oxide semiconductor (and logic family)
CMS	Center for Medicare and Medicaid Services
COB	Chip-on-board
COC	Cyclic olefin copolymers
COC	Chip-on-chip
COE	Computer order entry
COPD	Chronic obstructive pulmonary disease
CPT	Current procedural terminology
CRU	Constitutional repeating unit
CSF	Cerebral spinal fluid
CT	Computed tomography
DARPA	Defense Advanced Research Projects Agency
dc	Direct current
DEP	Dielectrophoresis
DHHS	Department of Health and Human Services
DNA	Deoxyribonucleic acid
DRIE	Deep reactive ion etching
DTM	Decal transfer microlithography
DTRA	Defense Threat Reduction Agency
EAC	Electroactive ceramic
EAP	Electroactive polymer
ECD	Electrochemical detection
EDL	Electric double layer
EG	Electronic grade silicon
EGDMA	Ethylene glycol dimethacrylate
EIS	Electrolyte-insulator-semiconductor
ELISA	Enzyme-linked immunosorbent assay
EnFET	Enzyme FET
EOF	Electro-osmotic flow
ESA	Electrostatic self-assembly
ESD	Electrospray deposition
ESI	Electrospray ionization
ESI-TOF MS	Electrospray ionization and time-of-flight mass spectrometry
ESSP	Electrostatically stricted polymer
EST	Expressed sequence tags
EUV	Extreme ultraviolet
eV	Electron volt
EWOD	Electrowetting-on-dielectric
FAME	Fatty acid methyl esters
FBGC	Foreign body giant cell

FCC	Face-centered cubic
FCC	Federal Communication Commission
FDA	Food and Drug Administration
FET	Field effect transistor
FHIT	Fragile histidine triad
FPW	Flexural plate wave
FSO	Full scale output
GGP	Good guidance practices
GMP	Good manufacturing practice
GPMT	Guinea pig maximization test
HBV	Hepatitis B virus
HCC	Hepatocellular carcinogens
HDE	Humanitarian device exemption
HDL	Alpha (high-density) lipoproteins
HEMA	2-hydroxyethyl methacrylate
HEXSIL	Hexagonal honeycomb polysilicate
HF	Hydrofluoric acid
HGF	Hepatocyte growth factor
HIV	Human immunodeficiency virus
HMM	Hidden Markov models
HMO	Health maintenance organization
HTO	High-temperature oxidation
HTS	High-throughput screening
HUPO	Human proteome organization
IBM	Ion-beam milling
ICP	Intracranial pressure monitoring
IDT	Interdigital transducers
IEEE	Institute of Electrical and Electronic Engineers
IFE	Interfacial free energy
IMS	Ion-mobility spectrometer
INR	International normalized ratio
IPMC	Ionic polymer-metal composite
IR	Infrared
IRB	Institutional Review Board
ISE	Ion-selective electrodes
ISFET	Ion-selective field effect transistor
ISO	International Standards Organization
ITO	Indium-tin-oxide
IUPAC	International Union of Pure and Applied Chemistry
JCAHO	Joint Commission on Accreditation of Healthcare Organizations
KOH	Potassium hydroxide
LADI	Laser-assisted direct input
LAT	Latex agglutination test
LC	Liquid chromatography
L-C	Impedance-capacitive

LCE	Liquid crystal elastomer
LC-MS	Liquid chromatography–tandem mass spectrometry
LDL	Beta (low-density) lipoproteins
LED	Light-emitting diode
LIGA	Lithography-electroplating-molding
LOC	Lab-on-a-chip
LPCVD	Low-pressure chemical vapor deposition
LTO	Low-temperature oxidation
MAc	Methacrylic acid
MALDI-TOF MS	Matrix-assisted laser desorption/ionization–time of flight mass spectrometry
MAUDE	Manufacturer and user facility device experience
MB	Molecular beacon
MBAAm	Methylenebisacrylamide
MDAC	Medical Devices Advisory Committee
mDNA	Mitochondrial DNA
MDR	Medical device reporting
MDUFMA	Medical Device User Fee and Modernization Act
MEMS	Microelectromagnetic systems
MGS	Metallurgic grade silicon
MIMIC	Micromolding in capillaries
MIS	Minimally invasive surgery
MIST	Multiple spotting technique
MOS	Metal oxide semiconductor
MOSFET	Metal oxide semiconductor field effect transistor
MPE	Maximum permissible exposure
MRI	Magnetic resonance imaging
mRNA	Messenger RNA
MS	Mass spectrometry
MSGC	Microstrip gas chamber
MSL	Micro stereolithography
MST	Microstructure technology
MWD	Molecular weight distribution
NA	Numeric aperture
NCCL	National Committee for Clinical Laboratory Standards
nDEP	Negative dielectrophoresis
NEGS	Nonevaporable getters
NIH	National Institutes of Health
NIL	Nanoimprint lithography
nTP	Nanotransfer printing
Nylon 66	Poly(hexamethylene adipamide)
OC	Office of Compliance
OCT	Optical coherence tomography
ODE	Offices of Device Evaluation
OIVD	Office for In Vitro Diagnostic Device Evaluation and Safety
OSB	Office of Surveillance and Biometrics

OST	Office of Science and Technology
OTS	Octadecyltrichlorosilane
PA	Polyamide (Nylon 6)
PAH	Poly(allylamine hydrochloride)
PANI	Polyaniline
PBT	Poly(butylene terephthalate)
PC	Poly(bisphenol A carbonate)
PCB	Printed circuit board
PCR	Polymerase chain reaction
pDEP	Positive dielectrophoresis
PDMS	Poly(dimethyl siloxane) or silicone
PDP	Product Development Protocol (FDA)
PE	Plasma etching
PE	Polyethylene
PEEK	Poly(ether ether-ketone)
PEG	Poyl(ethylene glycol)
PEM	Proton-exchange membrane
PEO	Polyethylene oxide
PET	Poly(ethylene terephthalate)
PET	Positron emission tomography
PETG	Poly(ethylene terephthalate glycol)
PI	Polyimide
PLGA	Poly(D.L-lactide-co-glycolide)
PMA	Premarket Approval (FDA)
PMMA	Poly(methyl methacrylate)
PMT	Photomultiplier tube
PNIPAAm	Poly(N-isopropylacrylamide)
PNIPAM	Poly(N-isopropylacrylamide)
PPM	Provider-performed microscopy
PPy	Polypyrrole
PS	Physical sputtering
PS	Polystyrene
PSF	Polysulfone
PSG	Phosphosilicate glass
PTFE	Poly(tetrafluoro ethylene)
PTM	Post-translational modification of proteins
PTT	Partial thromboplastin time
PVA	Poly(vinyl alcohol)
PVAC	Poly(vinyl acetate)
PVC	Poly(vinyl chloride)
PVD	Physical vapor deposition
PVDF	Poly(vinylidene fluoride)
PZT	Piezoelectric lead zirconate titanate
QCM	Quartz crystal balance
RAIRS	Reflection-absorption infrared spectroscopy
RBC	Red blood cells

RF	Radio frequency
RIBE	Reactive ion-beam etching
RIE	Reactive ion etching
RLS	Rotated light scattering
RNA	Ribonucleic acid
rRNA	Ribosomal RNA
RS	Raman spectroscopy
RT-PCR	Reverse transcriptase PCR
RWV	Rotating wall vessel bioreactor
SAM	Self-assembled monolayer
SAR	Specific absorption rate
SAW	Surface acoustic wave
SAXS	Small-angle x-ray scattering
SB/CCOM	Soldier Biological and Chemical Command
SC	Simple cubic
SCREAM	Single-crystal reactive etching and metallization
SELDI-TOF MS	Surface-enhanced laser desorption/ionization–time of flight Mass spectroscopy
SEM	Scanning electron microscope
SERRS	Surface-enhanced resonance Raman scattering
SH SAW	Shear horizontal surface acoustic wave
SIS	Reversible soluble-insoluble polymers
SL	Stereo lithography
SMA	Shape-memory alloy
SMD	Surface-mounted device
SNP	Single nucleotide polymorphisms
SOG	Silicon-on-glass
SOI	Silicon-on-insulator
SOS	Silicon-on-silicon
SPIE	The International Society for Optical Engineering
SPP	Surface plasmon polariton
SPRS	Surface plasmon resonance spectroscopy
ssDNA	Single stranded DNA
STOMP	Synthesis and transfer of materials to and from polymers
TE	Thickness expansion
TEM	Transmission electron microscope
TEOS	Tetraethylorthosilicate
Tg	Glass transition temperature
TNT	Trinitrotoluene
TOAB	Tetraoctadecylammonium bromide
TPLC	Total product life cycle
tRNA	Transfer RNA
TS	Thickness shear
TTL	Transistor-transistor logic
twDEP	Traveling wave dielectrophoretic force
UL	Underwriters Laboratory